



**GeoEarthScope**  
**InSAR Working Group Report**

September, 2006



# GeoEarthScope

## InSAR Working Group

### Report of planning meeting

**Boulder, CO July 11-12, 2006**

Yuri Fialko, UCSD, [yfialko@ucsd.edu](mailto:yfialko@ucsd.edu) (Chair)  
Falk Amelung, Univ. of Miami, [amelung@rsmas.miami.edu](mailto:amelung@rsmas.miami.edu)  
Ben Brooks, Univ. of Hawaii, [bbrooks@soest.hawaii.edu](mailto:bbrooks@soest.hawaii.edu)  
Jeff Freymueller, Univ. of Alaska, [jeff@giseis.alaska.edu](mailto:jeff@giseis.alaska.edu)  
Francisco Gomez, Univ. of Missouri, [fgomez@missouri.edu](mailto:fgomez@missouri.edu)  
Tim Melbourne, Central Washington Univ., [tim@geology.cwu.edu](mailto:tim@geology.cwu.edu)  
Kurt Feigl, Univ. of Wisconsin, [feigl@geology.wisc.edu](mailto:feigl@geology.wisc.edu)  
Gilles Peltzer, UCLA, [peltzer@ess.ucla.edu](mailto:peltzer@ess.ucla.edu)  
Gerald Bawden, USGS, [gbawden@usgs.gov](mailto:gbawden@usgs.gov)  
Craig Dobson, NASA, [craig.dobson-1@nasa.gov](mailto:craig.dobson-1@nasa.gov)  
Andrea Donnellan, NASA, [andrea.donnellan@jpl.nasa.gov](mailto:andrea.donnellan@jpl.nasa.gov)  
Zhong Lu, SAIC/USGS, [lu@usgs.gov](mailto:lu@usgs.gov)

## Summary

Interferometric Synthetic Aperture Radar (InSAR) technique has been identified by the science community as one of the essential components of EarthScope because InSAR can uniquely map and resolve surface deformation over a wide range of spatial scales that is not possible with any other geodetic technique. By combining InSAR with PBO GPS and strainmeter measurements, one can comprehensively quantify spatial and temporal characteristics of deformation across the Pacific and North American plate boundary in the United States. GeoEarthScope can provide the means of fulfilling this major objective of the greater EarthScope initiative. The US research community currently relies on InSAR data collected by several radar satellite missions, including those flown by the European (*ERS-2*, *Envisat*), Canadian (*Radarsat-1*) and Japanese (*ALOS*) Space Agencies. This report describes a plan for the acquisition of InSAR data through GeoEarthScope.

The InSAR Working Group is making the following recommendations for GeoEarthScope that address satellite tasking, target prioritization, the acquisition of historical archive data, and the management and distribution of SAR data to the broader science community.

- *Tasking* – Frequent and persistent acquisitions of InSAR data are crucial for accurate measurements of small strain signals associated with interseismic and postseismic deformation, as well as for a rapid and efficient response in case of major natural disasters like earthquakes or volcanic eruptions. The InSAR Working Group recommends that the InSAR data be collected on every satellite pass in the identified high-priority areas, with acquisitions from both the ascending and descending satellite orbits. Currently, *Envisat* does *not* routinely collect SAR imagery across most of the GeoEarthScope targets as the *ERS1/2* satellites have done. It is now necessary to obligate financial resources to ‘turn on’ the satellites such that data will be collected; otherwise, there will be no data for the research community to analyze.
- *Satellites* – Observations from different orbits and imaging modes enable one to resolve an intrinsic ambiguity between the vertical and horizontal components of motion for a 3-D recovery of the surface displacement field. We propose acquiring new data in a “standard *ERS*-like” imaging mode for the *Envisat* satellite, and an imaging mode with shallower incidence angles for the *Radarsat-1* satellite. In addition, the Working Group expresses a strong interest in use of data from the L-band *ALOS* satellite recently launched by the Japanese Space Agency because the longer wavelength of the *ALOS PALSAR* instrument will allow interferometric measurements in areas with more extensive vegetation and precipitation where the traditional C-band interferometry has been problematic (for example, along the northern and central sections of the San Andreas fault).
- *Target Prioritization* – The target selection and prioritization was optimized to provide the maximum spatial and temporal coverage to support the diverse scientific needs of the GeoEarthScope community, address the major EarthScope science drivers, and to complement PBO siting and data analysis. The targeting includes: the San Andreas fault system, the Eastern California Shear Zone, Basin and Range, the Mendocino Triple Junction, volcanoes, active crustal faults and the subduction zones in Cascadia and Alaska, and a number of distributed targets across the United States including the Rio

- Grand Rift, New Madrid, Charleston, Galveston, and New Orleans.
- *Historic Archive Data* – The InSAR Working Group recommends that UNAVCO works with the European Space Agency to purchase the *ERS-1*, *ERS-2* and *Envisat* archive data for the targeted regions. This will provide in some regions close to a 15-year archive of land surface change and will have an archive set of sufficient coverage to begin evaluating continental-scale deformation.
  - *Data Management* – UNAVCO needs to develop and implement: 1) a subsystem for data delivery to GeoEarthScope, with a data search and order interface that includes selection by baselines values and an on-line L0 archive in a specified format; and 2) a procedure for near real time (NRT) acquisition and processing for future *Envisat*, *ALOS*, *Radarsat-1* etc. data in the event of an earthquake. This includes negotiating foreign station NRT L0 delivery to the UNAVCO on-line archive as well as utilizing existing ground stations in the US having the ability to downlink SAR data.

This report also outlines perspective directions in the InSAR research that ought to be facilitated by GeoEarthScope, including permanent scatterer interferometry, ScanSAR, UAVSAR, and use of auxiliary data such as water vapor measurements in the atmosphere. The acquisition plan outlined in this report will provide an InSAR component to EarthScope, and lead to major advances in our understanding of deformation processes (both natural and anthropogenic) and their associated hazards.

## **Table of contents**

1. Introduction	p.5
2. Scientific rationale for regular and repeated acquisitions of SAR data	p. 6
3. Science drivers: Major geographic and tectonic targets of EarthScope/PBO	p.10
4. Future challenges and scientific justification for continued data acquisitions	p. 20
5. Data requirements	p. 27
6. New and emerging technology	p. 30
7. Budget justification	p. 33
8. References	p. 34

## 1. Introduction

Interferometric Synthetic Aperture Radar (InSAR) is one of the most important and exciting recent developments in observational geophysics that has revolutionized (along with the Global Positioning System) disciplines of space geodesy, crustal deformation, and active tectonics. Space-based geodetic observations provide detailed information about the surface deformation due to natural and anthropogenic causes. These observations are essential for understanding deformation of the tectonic plates and the fluid behavior of the mantle below. Over the last decade, InSAR has proven itself as a valuable tool for detecting and monitoring changes in the Earth's surface due to seismic, volcanic, tectonic, hydrologic etc. activities, and forecasting a variety of natural hazards. For example, observations of deformation from subsurface flow of magma and of the accumulation of tectonic strain within the crust are needed for understanding of volcanic and seismic phenomena. More localized, but often intense, hazards include landslides, mud flows and land subsidence or collapse due to natural or human removal of subsurface material or fluids and permafrost melting. Flooding is the most damaging hazard in most areas, from rainfall, snow and ice melting, and natural or human-made dam collapse. In coastal regions, hurricanes, intense local wind events, shore erosion and oil spills are major hazards. Finally, fire in forests and other vegetation is a major hazard in many areas. For each of these hazards, InSAR is capable of providing help in assessing damage after the events and evaluating the risk of future events by understanding and monitoring the processes involved. Overall, InSAR observations provide critical and otherwise unavailable data enabling comprehensive, global measurements to better understand and predict changes in the Earth system.

One of the most powerful features of InSAR is its ability to generate continuous high-resolution maps of surface strain over large areas and at any weather or day/night condition, with a modest cadency (typically, on monthly timescales). This makes InSAR a highly complementary and synergetic technique with the Plate Boundary Observatory's networks of the Global Positioning System (GPS) and strain meter instruments, and an indispensable tool for achieving the objectives of EarthScope. The National Research Council 2001 "Review of EarthScope Integrated Science" characterized InSAR as "an essential component of the EarthScope Initiative." Given that the US InSAR satellite mission is only in the intermediate stages of planning, the EarthScope research community requires access to the Synthetic Aperture Radar data collected by the existing InSAR-capable satellites. This report outlines a plan for the acquisition of SAR data through GeoEarthScope. This acquisition plan will satisfy most of the data demand by the science community, and provide an InSAR component to EarthScope.

InSAR has already become a primary tool for measuring coseismic deformation and postseismic transients (provided adequate coverage). Accurate and robust measurements of subtle secular and precursory deformation are the new frontiers in the crustal deformation studies, and are also pivotal for the solid Earth natural hazards research. Detecting and quantifying small strain signals require massively redundant interferograms to beat down the noise and alleviate the effects of decorrelation. This implies frequent and persistent data takes over the target areas. Ultra-precise and spatially dense data are of critical importance to studies of earthquake slip, postseismic deformation, and the mechanical behavior of faults, issues of fundamental scientific importance. These data will also benefit society through improved understanding of earthquake hazards. Current earthquake hazard maps, the principal hazard estimate used by planners and

engineers, are at a coarse resolution in both time and geography. Such maps depict probability of exceeding a certain amount of shaking (generally that at which damage occurs) over the next 30 to 100 years, depending on the map. The spatial resolution is typically on the order of tens to hundreds of kilometers. These maps are based on information about past earthquakes observed in the geological or historical record. Measurements of crustal deformation, usually acquired using GPS, now provide information on strain rates, and generally there is evidence that earthquake rates are higher where strain rates are higher. The large number of GPS stations that will be deployed on the ground under the auspices of PBO requires validation and site characterization that can be readily provided by InSAR. InSAR deployed as a space-based imaging technique provides spatially smooth resolution of strain at 100 m, vastly improving resultant hazard estimates by two to three orders of magnitude in terms of spatial resolution. Furthermore, future studies of crustal deformation will yield insights into earthquake behavior, whether high strain rates indicate the initiation of failure on a fault or quiet release of stress, and how stress is transferred to other faults. These studies will lead to science findings for improvement of earthquake hazard maps both spatially and temporally.

InSAR imagery has been an integral part of the Plate Boundary Observatory (PBO) GPS site selection process to ensure that the sites are located in areas with little known natural or human-induced surface motion associated with subsurface fluid flow [Bawden *et al*, 2005; Walls *et al*, 2006] and is needed to fully characterize the GPS time-series data from the entire PBO footprint. Natural variations in ground-water levels and the ever-changing management of ground water, hydrocarbon, and geothermal resources throughout the western United States produce large-scale surface deformation that is directly measured in both horizontal and vertical GPS components. InSAR imagery is often the only technique that can fully characterize the spatial signature and magnitude of non-tectonic deformation source such that it can be removed to provide a sound geophysical understanding of the area of interest. Over half of the GPS sites in Los Angeles Basin show anthropogenic signal in the GPS time-series and the increasing demand for water in the west is changing the ground-water pumping practice such that sites that were once stable may have anthropogenic contributions in their time series. Routine collection of SAR imagery in the PBO footprint is essential to fully characterize deformation at PBO sites and to ensure the success of PBO, especially in regions with a sparse PBO site distribution and in low strain rate regions where ground water pumping can overwhelm the sought-after signal.

## **2. Scientific Rationale for Regular and Repeated Acquisitions of SAR Data**

Geodetic observation strategy in seismic areas is motivated by models of the earthquake cycle [e.g., Tse and Rice, 1986, Figure 1]. Above a depth of about 30 km, plate boundary deformation is primarily accommodated on discrete faults. Within the seismogenic zone (depth < 12-15 km), sliding is episodic because the static coefficient of fault friction is greater than the dynamic coefficient of friction (*velocity weakening*) [Tse and Rice, 1986]. At greater depths, slip is steady state because the friction on the fault increases with sliding velocity (*velocity strengthening*). The time and depth variations in slip depend on a number of poorly constrained model parameters as well as the orientation and intensity of the applied stress field. Geodetic measurements can reveal the distribution of surface strain with distance from the fault and thus can be used to infer the slip distribution with depth [Rundle and Jackson, 1977; Thatcher, 1983;

*Turcotte and Schubert, 2002; Lorenzetti and Tullis, 1989; Savage, 1990*]. Networks of seismometers, GPS antennae, and other geodetic instruments provide exceptional temporal coverage of the co-seismic, post-seismic, and inter-seismic motions in the PBO area, but their spatial coverage is often insufficient. Interferometric synthetic aperture radar complements these systems by providing complete 100-m spatial resolution but at a much lower sampling interval (of the order of several weeks or more). It is critical to have a SAR data acquisition plan in place prior to a major earthquake. This requires paying the appropriate space agency to task the satellite and to acquire a large quantity of those data.

Perhaps the most vivid illustration of a successful acquisition strategy is the case of the 1999 Hector Mine Earthquake, which we use as an example of the use of a rich InSAR data set to study earthquakes. A variety of instrumentation and investigations were used to obtain a rather complete understanding of this major earthquake [*Rymer et al., 2002*]. The observations include: prior geologic mapping to locate faults and assess their paleo-activity, seismology for measuring pre-seismic, co-seismic and post-seismic activity as well as to establish the rupture dynamics of the main event; GPS (both continuous and campaign) to measure vector motions with good temporal resolution and moderate spatial coverage; geologic and geodetic field programs after the event to measure co-seismic and triggered slip; as well as InSAR to provide very dense spatial coverage to measure co-seismic and post-seismic deformation.

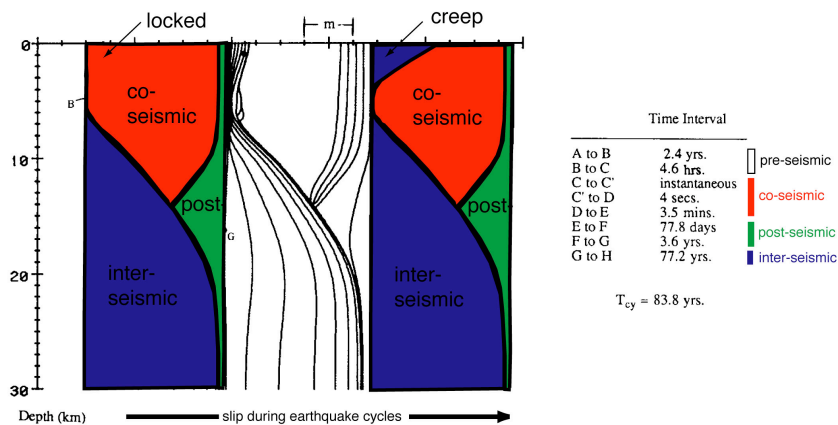
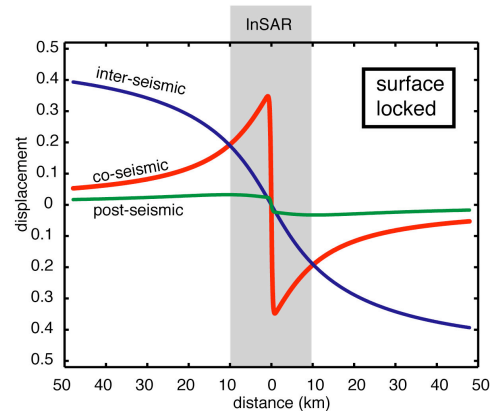


Figure 1. (above) fault slip versus depth for three complete earthquake cycles after *Tse and Rice [1986]*. At each depth, the sum of the pre-, co-, post- and inter-seismic slip must equal the geologic displacement.

(right) surface displacement across the fault for the co-, post- and inter-seismic parts of the cycle. At each distance from the fault, the sum of the displacements must equal the geologic displacement.

InSAR is the best tool for monitoring near-field co- and inter-seismic displacement over large areas. GPS is the best tool for monitoring post-seismic displacement.



The InSAR technique is highly complementary to the PBO GPS and strainmeter instrumentation, and, as described below, offers unique insight into the earthquake cycle.

The Hector Mine earthquake was extraordinarily well imaged by the *ERS-2* spacecraft for a number of reasons:

- First, pre-allocated resources from the funding agencies were used to schedule the monthly data acquisitions along the entire SAF system for 4 months prior to and 12 months following the event. (Continued post-seismic acquisitions were halted in late 2000 when the gyroscopes aboard *ERS-2* satellite failed.) ESA was able to acquire most of the descending tracks requested and about 1/3 of the ascending requested. This is unusual because, for most parts of the world, a nominal data acquisition schedule is once or twice per year. Since the orbit of the *ERS-2* satellite is controlled in a 2000 m diameter tube it typically takes 10-20 repeat orbits (1-2 years) to match a reference orbit to within the desired 100 m baseline. Thus the number of pre-earthquake acquisitions usually determines the minimum time span of an interferometric match.
- In the case of the Hector Mine earthquake, the descending co-seismic pair has the minimum possible time span of 35 days, it was acquired just 4 days after the event, and it also has an extraordinarily short baseline of only 18 m. This short baseline is not a fluke of statistics but rather an effort by the European Space Agency to control the satellite orbit to optimize data collection.
- Finally, the Mojave Desert, with low vegetation and low rainfall, is an ideal surface for retaining interferometric coherence over time spans of 8 years or more. High coherence enables one to probe the shortest wavelengths in the interferometric phase to reveal the details of the rupture.

*Co-seismic vector displacement due to Hector Mine rupture* - The nearly optimal co-seismic InSAR observations provided, for the first time, continuous 3-D vector displacements that showed good agreement with the more widely-spaced GPS measurements [Fialko *et al.*, 2001a] (Figure 2) and geologic mapping of the surface rupture. These combined GPS/InSAR data were inverted for the slip distribution at depth [Simons *et al.*, 2002; Jonsson *et al.*, 2002] with much greater detail than could be obtained from the available seismic and GPS measurements. The inversion revealed a remarkably detailed picture of the co-seismic motion including an enigmatic shallow slip deficit that may suggest distributed inelastic yielding in the upper few kilometers of the crust during the earthquake or in the interseismic period. Furthermore, analysis of the interferometric correlation revealed parts of the surface rupture that went unnoticed in the detailed ground-based surveys [Simons *et al.*, 2002].

*Fault deformation induced by nearby large earthquakes* - One of the most intriguing observations from the co-seismic interferograms was the prevalence of strain lineaments adjacent to the main rupture [Sandwell *et al.*, 2000]. Induced strain occurs on the previously mapped, parallel faults [Jennings, 1994] and the sense of displacement switches polarity according to the lobate structure of the stress field due to the main rupture, suggesting that this may reflect a local amplification of the co-seismic strain rather than a triggered response to existing tectonic stress. On the southwest side of the main rupture, the southern strands of sub-parallel faults (i.e., Emerson, Hidalgo, and West Calico) all display a few mm of right-lateral offset. In contrast the northern strands of the connecting faults (e.g. Calico and Rodman) display a few mm of left-lateral offset or west-side-up offset. An ascending interferogram was used to confirm the left-lateral strain (opposite to the regional stress field). The most reasonable explanation is the response of compliant fault zones to permanent co-seismic stress changes [Fialko *et al.*, 2002].

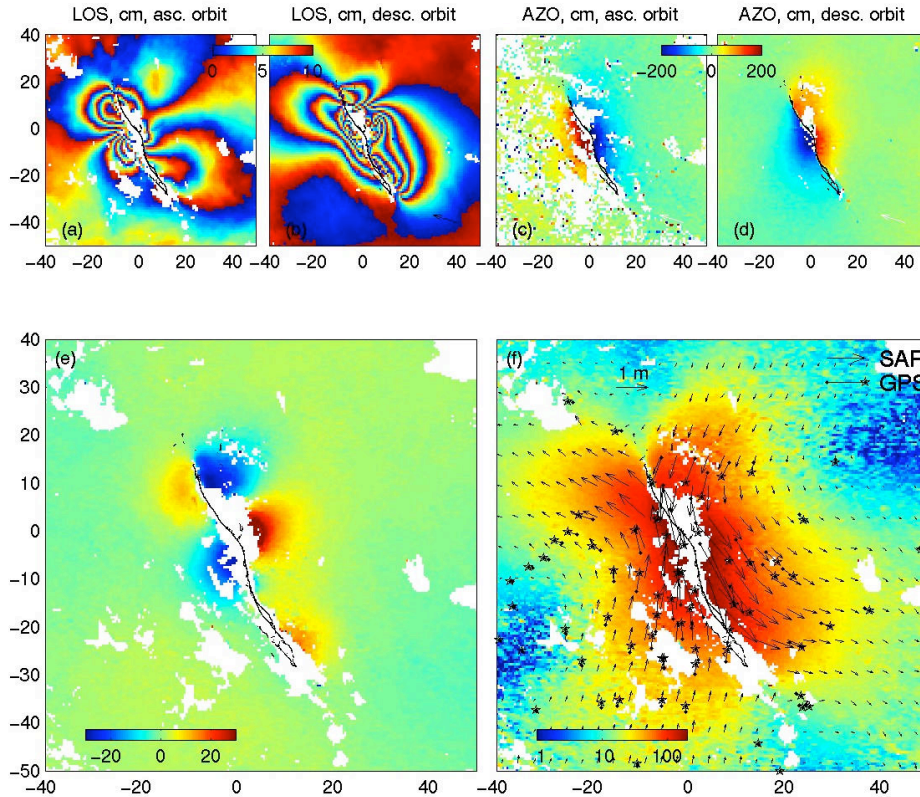


**Figure 2.** *ERS* interferometry provided measurements of four projections of surface displacement – ascending track (a,c), and descending track (b, d) – that can be uniquely transformed into three Cartesian components, vertical (e), and horizontal (f). Comparison of these vector measurements with GPS data shows good agreement at the 5 cm level [Fialko *et al.*, 2001a].

The induced fault displacements imply decreases in the effective shear modulus within the kilometer-wide fault zones.

*Post-seismic relaxation following Hector Mine Earthquake* – The *ERS-2* pass collected just 4 days after the Hector Mine Earthquake was critically important for studying post-seismic processes since a large fraction of post-earthquake deformation may occur within the first few months after the main shock [Shen *et al.*, 1994; Massonnet *et al.*, 1996]. For much larger events, such as the 2002 Denali fault earthquake, the fraction of post-earthquake deformation occurring within the first few months is smaller [Pollitz *et al.*, 2003; Freed *et al.*, 2006], but also in these cases the first few months contain critical time variations in the deformation signal that constrain the deformation mechanisms. There have been several analyses of the post-seismic displacement following the Hector Mine event. Postseismic deformation in the near field reveals deformation consistent with shallow afterslip and fault zone collapse [Jacobs *et al.*, 2002]. The timescale of this deformation is 135 days, which is consistent with the near-field deformation following the Landers 1992 event [Shen *et al.*, 1994]. The cause of the far-field post-seismic deformation is still a matter of debate. Pollitz *et al.*, [2001] used the vertical deformation derived from InSAR to suggest that deep afterslip is not a viable model (Figure 3). They argued for transient flow in the upper mantle. While the cause of this deformation is still uncertain, the SAR data acquisition on October 20, just 4 days after the earthquake was key to revealing these processes. This track

probably would not have been acquired without the standing order from the US research community (WInSAR consortium).

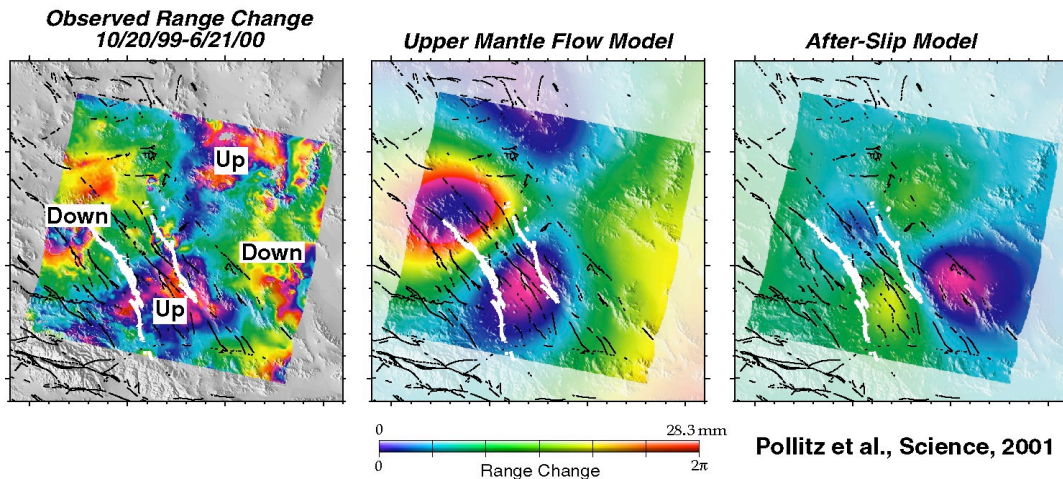


**Figure 3.** Postseismic displacement following the Hector Mine earthquake from *Pollitz et al.* [2001] shows that the deep after slip model is inconsistent with the vertical deformation. Recent poroelastic models are also consistent with the observed deformation pattern although *Pollitz et al.*, [2001] favor the upper mantle flow model.

*San Simeon Earthquake* – In contrast to the excellent InSAR coverage of the 1999 Hector Mine event, InSAR coverage of the December 22, 2003 San Simeon was poor. No acquisition plan for either *Envisat* or *Radarsat-1* was in place when the earthquake occurred so the most critical data just prior to, and just following the earthquake were not acquired.

*Denali Earthquake* – InSAR coverage of the November 3, 2002 Denali earthquake in Alaska was mixed. The earthquake occurred after the failure of key components of ERS-2, but before Envisat was available. There was no systematic pre-earthquake coverage of the region from the Radarsat-1 satellite, the only SAR satellite available at that time. Many scenes were available for one track that corresponded to the Trans-Alaska Oil Pipeline, and limited data from the western 1/3 of the rupture, but no coseismic interferograms could be produced for the eastern half of the 326-km-long rupture. The GeoEarthScope InSAR Working Group recommends that the acquisition plan includes tasking of currently available InSAR platforms in preparation for the next major event.

### 3. Science drivers: Major geographic and tectonic targets of EarthScope/PBO

#### *The San Andreas Fault System*

The San Andreas fault (SAF) in California is a major plate boundary fault that accommodates much of relative motion between the Pacific and North America. Except for the 140-km long fault section between Parkfield and San Juan Batista that undergoes a steady creep, the SAF exhibits a stick-slip behavior, and is capable of producing great earthquakes. The two most recent great earthquakes on the SAF have ruptured its northern and central sections in 1906 and

1857, respectively. The southern section of the fault has not produced a great earthquake in historic times (over more than 300 years), but geologic and geodetic data indicate that it did rupture in the past, and accumulates substantial elastic strain at present. Frequent InSAR observations of the 1000-long San Andreas fault are crucial for advancing our knowledge about the rate and style of the secular interseismic build-up of strain, and ensuring that suitable pre- and post-earthquake acquisitions are available in case of a major event. Major outstanding questions concern slip rates and locking depths on various segments of the SAF, as well as other faults comprising the San Andreas Fault system, the prevalence and magnitude of surface creep, and 3-D variations in the mechanical properties of the Earth's crust. Spatially and temporally dense InSAR observations will also allow us to resolve the critical issue of precursory deformation (or lack of thereof), as well as the on-going debate about the mechanisms of post-seismic relaxation. Figure 4 illustrates the imaging capabilities of InSAR in application to the slow interseismic deformation. The line-of-sight (LOS) velocity field in Figure 4 clearly reveals the relative motion between the Pacific and North American plates. The InSAR-derived deformation rates indicate a nearly equal partitioning of strain on the San Andreas and San Jacinto faults, and are in excellent agreement with independent ground-based measurements [Fialko, 2006]. Due to a lack of significant (moment magnitude greater than 7) historic earthquakes on the southern SAF, and portions of the San Jacinto fault (e.g., the Anza gap), these faults are currently believed to pose the largest seismic hazard in California. Similar results can be derived for the central and northern sections of the SAF, although those areas are less favorable for interferometry due to vegetation and precipitation. Frequent acquisitions, as well as use of L-band *ALOS* data may substantially alleviate these problems. The northern section of the SAF system, in particular, from the creeping section to the Mendocino Triple Junction, is just as

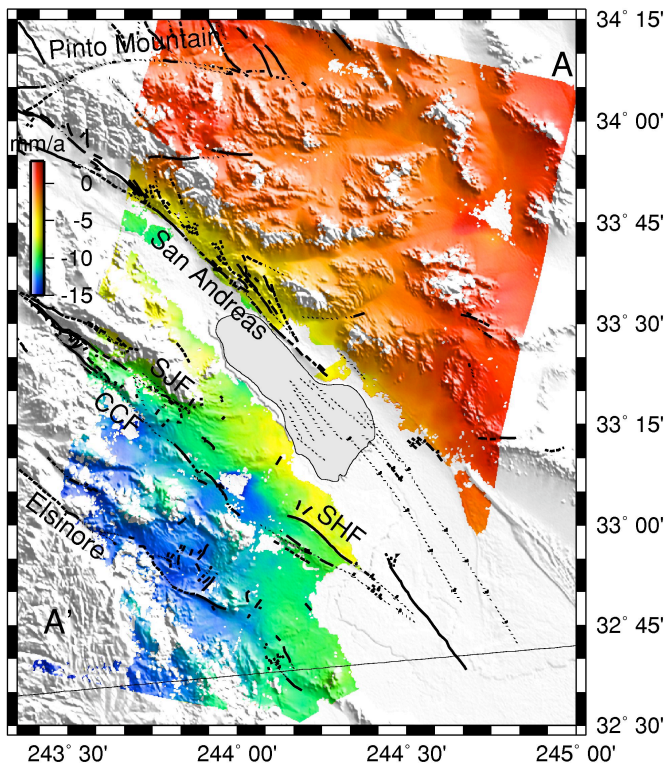


**Figure 4.** Line of sight velocity of the Earth's surface, in millimeters per year, from a stack of ~40 radar interferograms spanning a time interval between 1992 and 2000. The velocity map is draped on top of shaded topography. LOS velocities toward the satellite are assumed to be positive. Black wavy lines denote Quaternary faults (SJF - San Jacinto fault, CCF - Coyote Creek fault, SHF - Superstition Hills fault). From *Fialko* [2006].

complex as the southern section, but except in urbanized areas will require L-band *ALOS* data and/or improved analysis techniques (such as Permanent Scatterer InSAR, or PSInSAR) to produce comparable results.

### *The Eastern California Shear Zone*

The 100 km-wide Eastern California Shear Zone trends  $\sim$ N24°W from the eastern end of the Transverse Range into the Walker Lane. While the faults that constitute the ECSZ have long been recognized by geologists, it is on the basis of geodetic observations that the ECSZ was revealed as a zone of concentrated shear taking into account up to 20-30% of the Pacific-North America plate motion. The setting, structure, and seismic history of the ECSZ are complex in many respects making it an exceptional case to study processes associated with the inter-seismic stress loading, the generation of earthquakes, and the relaxation processes taking place subsequent to their occurrence. The ECSZ is therefore a prime target to be covered with InSAR data in the GeoEarthScope effort.

1. The ECSZ has been the locus of the largest three earthquakes in Southern California in the last 135 years (Owens Valley, M 7.8, 1872, Landers, M 7.3, 1992, Hector Mine, M 7.0, 1999). These earthquakes have significantly affected the regional stress field triggering relaxation processes in the crust and upper mantle. Monitoring with InSAR the surface deformation in the Mojave and western basin and Range area is essential to understand crustal properties, the processes involved in post-seismic phases, and how the stresses are re-adjusted after large events.
2. The ECSZ crosses the Garlock fault and is probably responsible for the gradual bending of the fault to the south along its eastern 100 km-long section (Figure 5). Geodetic observations indicate that right-lateral shear integrated across the shear zone is apparently uniform from south to north [*Savage et al.*, 1990]. Cumulative, right-lateral slip on many of the faults forming the ECSZ has been documented both north and south of the Garlock fault from geological data. Yet, none of the faults in the shear zone approaching the Garlock fault actually cut it. We may therefore be witnessing a critical moment in the geological history of the shear zone, when new fault segments will finalize the connection between the north and south faults across the Garlock fault. Monitoring the surface deformation associated with the transfer of stress between conjugate faults is critical to understand fault evolution in complex continental settings.
3. The ECSZ is composed of many distinct fault segments, which interact between each other. For example, the occurrences of two M 7+ earthquakes, seven years apart, on two parallel faults separated by 20 km (Landers and Hector Mine) must have been influenced by the stress change produced by the first event. Similarly, the narrow zone of concentrated shear along the Blackwater fault revealed by InSAR data may result from the interaction between this fault and other structures such as the Garlock fault or other sections of the ECSZ in line with the Blackwater fault, which broke in recent earthquakes (Owens Valley, 1872 and Landers, 1992). Understanding these processes requires spatially and temporally dense deformation measurements that InSAR time series data can provide.

The *ERS*, *Envisat*, *Radarsat*, and *ALOS* SAR data archive assembled in the GeoEarthScope project will provide scientists with unprecedented means of investigation into these fundamental

questions. It will also help design the ultimate configuration of the future NASA SAR mission, the first of a kind dedicated to earthquakes and crustal deformation studies.

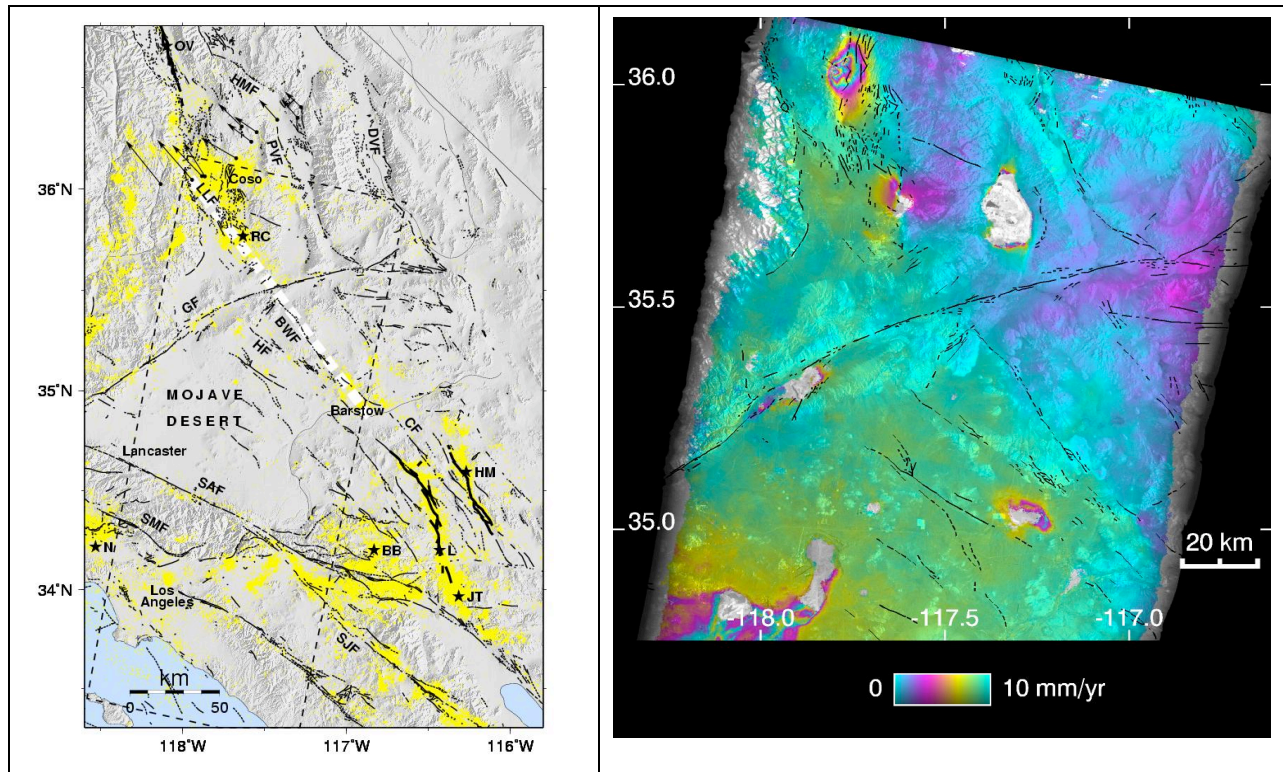


**Figure 5.** Left: Map of Mojave area showing major faults (black lines), seismicity (yellow dots), and surface rupture of recent earthquakes (thick lines). Arrows in north part of map are GPS velocity from *Gan et al.* [2000]. White dashes indicate location of localized shear observed in InSAR data. GF: Garlock Fault, BWF: Blackwater Fault, L: Landers, OV: Owens Valley. Right: Average line of sight velocity map over northern Mojave area obtained by stacking 25 interferograms acquired by ERS satellites between 1992 and 2000 [*Peltzer et al.* 2001]. Colors indicate ground movement component towards satellite.

### *Basin and Range*

The Basin and Range Province, located between the Sierra Nevada and the Coast Ranges in the east and the Rocky Mountains and the Colorado plateau in the west may accommodate up to 25% of the relative plate motion between the North American and the Pacific plates. GPS data acquired over the last 15 years suggest that most of the deformation is localized along its margins, on the Wasatch fault in the east and in the Walker Lane in the west. A distinct zone is the Central Nevada Seismic Belt which is characterized by elevated seismicity and generated several magnitude >7 earthquakes in the past century.

The major science issues for the Basin and Range geodynamics are:

1. Is active crustal deformation confined to the eastern and western Basin and Range as suggested by the existing, spatially sparse GPS data? This would imply that the Central Basin and Range is a micro plate that currently does not experience any deformation.

2. What is the nature of deformation of the Walker Lane in the western Basin and Range and what are the driving forces for this deformation? Is this region an incipient plate boundary that

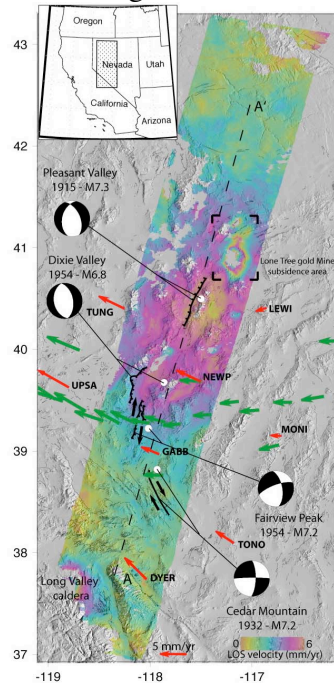


**Figure 6.** 1992–2000 LOS velocity map for the area of the 1915–1954 Nevada earthquakes together with epicenters (blank circles), focal mechanisms (spheres), and surface ruptures. Green arrows, campaign GPS velocities; red arrows, Basin and Range Geodetic Network (BARGEN) permanent GPS velocities. From *Gourmelen and Amelung* [2005].

eventually will supercede the San Andreas system as the major plate boundary between the Pacific and North American plates?

3. What is the nature of seismic activity in the Central Nevada Seismic belt? What is special about this region that could explain the elevated seismicity and heat flow?

The Basin and Range province has only sparse coverage by the Plate Boundary Observatory because of its large spatial extent. InSAR can fill this observational gap. An example of how InSAR can improve our understanding of the Basin and Range geodynamics is a stacked interferogram of the Central Nevada Seismic Belt (Figure 6). It shows subtle long-wavelength ground deformation of the order of 2–3 mm/yr that is consistent with models of mantle relaxation following a series of 50–80 year old major earthquakes [*Gourmelen and Amelung*, 2005].

### *Mendocino Triple Junction*

The Mendocino Triple Junction (MTJ) marks the boundary between the San Andreas System to the south and the Cascadia subduction zone to the north. Just as the San Andreas system consists of multiple faults distributed across a region, deformation associated with the triple junction is distributed across a broad region. In addition, because of the complexity of the Pacific–North America plate boundary zone, the MTJ deforming region reflects the interaction of several plates or blocks: the Pacific, Juan de Fuca and Gorda plates offshore, the Sierra Nevada–Great Valley and Oregon Coast forearc blocks onshore, as well as one or more slivers bounded by faults of the San Andreas system. GPS observations from the region [*Williams et al.*, 2006] show that margin-normal contraction is caused by a combination of subduction-related processes and impingement of the Sierra Nevada–Great Valley block onto the triple junction, and that both San Andreas-parallel shear and San Andreas-parallel contraction are associated with the northward

propagation of the San Andreas system into the Cascadia forearc. The broader MTJ region is a complex region, with active structures reflecting a combination of Cascadia subduction-related faulting and San Andreas system faulting. It offers an opportunity to study the development of very young strike-slip faults and the lateral propagation of a major transform system, as well as onshore examples of subduction-zone forearc structures that are submarine in most places. This region has not been a target of InSAR studies in the past, but new L-band *ALOS* data and new techniques like PSInSAR provide the opportunity for critical new insights.

### *Cascadia*

The Cascadia subduction zone occupies nearly half of the North America plate boundary in the lower 48 states. Considered aseismic by many earth scientists until two decades ago, paleoseismology now tells us that the 1,300 km-long Cascadia subduction zone has generated great earthquakes every 500-600 years on average, with a record that extends back at least 11,000 years [Atwater and Hemphill-Haley, 1997; Goldfinger *et al.*, 2003; Nelson *et al.*, 1996]. The most recent great earthquake, in 1700 AD, appears to have ruptured the entire plate boundary in a Mw 9 event [Satake *et al.*, 1996]. Cascadia's seismic moment release dwarfs other parts of the plate boundary outside of Alaska. Geodesy (leveling, precise gravity, laser ranging, GPS) repeated during the last 15-70 years indicates elastic strain accumulation in preparation for the next earthquake [Savage *et al.*, 1991; Dragert *et al.*, 1994; Mitchell *et al.*, 1994; Khazaradze *et al.*, 1999; McCaffrey *et al.*, 2000]. Like other subduction zones, Cascadia shows along-strike variations in elastic strain due to variations in the width and frictional behavior of the seismogenic zone [e.g., McCaffrey, 2002]. The Cascadia subduction zone strongly influences the kinematic and geodynamic behavior of the North American plate margin; yet we have only rudimentary knowledge of Cascadia's contemporary velocity field, its spatial and temporal variation, and its relationship to the subduction seismic cycle and tectonic driving forces.

Our proposed data acquisition plan (Figure 13) will help mapping the velocity and strain fields along the Cascadia convergent margin at the highest possible precision and resolution. Principal scientific objectives that drive this plan include: establishing the character and behavior of the Cascadia megathrust, including its along-strike variations, and its geodynamic role in western North America, determining the extent of strain partitioning in the convergent margin, and the role of continental extension, distributed transform faulting, contraction, and magmatism in accommodating deformation. Active forearc structures include the Seattle fault and other active faults that may threaten urban areas. The 1300-km-long Cascade volcanic arc is also the largest and most active volcanic system in the conterminous United States. Tracking magmatic processes and edifice instabilities requires high spatial and broad temporal strain resolution. Understanding interactions between magmatic and tectonic processes requires broad-scale deformation monitoring. The InSAR data are already revealing significant volcanic deformation that would have otherwise go unnoticed [Wicks *et al.*, 2002], and the proposed GeoEarthScope acquisition plan will greatly advance (in consort with the PBO deployments) our knowledge of the regional tectonics and magmatism of the Pacific Northwest, and the associated geohazards.

### *Alaska*

Alaska is by far the most seismically active region in the United States, primarily due to the active subduction of the Pacific Plate beneath the North American Plate (average convergence rates ~5 to 7 cm/year). Ten great earthquakes have occurred along the Aleutian trench since

1900. Alaska averages one M8 event every 13 years and one M7 event every year. M7 events are a possibility virtually anywhere in Alaska, and M6-7 events occur at a rate of at least 5 per year. The 2002 M7.9 Denali earthquake was the largest earthquake in the US over the last several decades. In addition, Alaska hosts most of active volcanoes in the US; about 2/3 of the historically active volcanoes are seismically monitored by the Alaska Volcano Observatory, but only a handful are instrumented for deformation measurements. For many active volcanoes in Alaska, InSAR data will be the only crustal deformation data available. Alaska also features the collision and active accretion of a fragment of continental crust, the Yakutat terrane, which is at least in part responsible for driving active faulting across a broad swath of southern and western Alaska, including the Denali fault system.

The Denali fault is a long, active strike-slip fault similar in length or longer than the San Andreas system, when its active segment in Canada and probably active (but almost completely unstudied) section in western Alaska are included. Unlike the San Andreas system, it developed not as the main actor in a broad, transform-dominated plate boundary zone, but inboard of and broadly parallel to a subduction zone. Unlike classic cases of slip partitioning like Sumatra, however, the sense of slip on the Denali fault over most of its length is opposite to that predicted by slip partitioning of oblique subduction. Slip on the Denali and related faults today is probably driven by the collision and accretion of the Yakutat terrane. In addition to the section of the fault that ruptured in the M7.9 2002 Denali fault earthquake, active segments of similar length stretch east and west and are capable of generating similar-sized earthquakes. Postseismic deformation from the 2002 earthquake has produced decimeters of postseismic deformation over a broad region around the fault, and a significant component of the postseismic deformation is decaying slowly with time [Freed *et al.*, 2006]. Postseismic deformation from the 2002 earthquake will produce substantial deformation, easily observed by InSAR, over at least the next few decades.

The Alaskan subduction zone also produces significant deformation over a broad region, due to the exceptionally shallow dip of the subducting plate and correspondingly wide locked seismogenic zone. This elastic component of deformation varies dramatically along-strike, due to along-strike variations in the frictional behavior of the subduction interface, which features alternating locked and creeping segments [Freymueller *et al.*, 2000; Zweck *et al.*, 2002]. At the boundary between these segments, the width of the frictionally locked portion of the subduction interface can change from >200 km to <50 km over an along-strike distance of 50 km or shorter. Because the plate convergence direction is sub-parallel to both the ascending and descending tracks (the angle between the two tracks decreases as one nears the pole), the deformation gradients associated with these variations in plate coupling may be the most straightforward target for InSAR. In addition, postseismic deformation from the 1964 Alaska (M9.2-9.3) earthquake continues to produce displacements of 5-20 mm/yr over an area about the size of California and Nevada combined.

The combination of PBO sites and InSAR imagery collected during the snow-free months (see Figure 14) will help determine the nature of the locked parts of the subduction interface, and a transfer of compressional forces originating from the collision of tectonic plates. The PBO and InSAR data will also significantly advance our understanding of a rheologic response of continental crust to a major strike-slip earthquake. InSAR data may also be able to image deformation caused by future slow slip events on the plate interface, if they are as large as the

1998-2001 event near Anchorage. Unlike the much smaller (and more frequent) Cascadia slow slip events, which produce millimeters of surface deformation, the much larger Alaska event produced total displacements of about a decimeter, embedded within a broad zone of steady strain. An InSAR time series approach would allow measurement and modeling of deformation from such events.

#### *Distributed Targets in the Central and Eastern United States*

Although often generalized as a “stable” continental interior, localized crustal deformation in the Central and Eastern United States (CEUS) presents scientific challenges to understanding continental dynamics. Broader geodynamic themes include understanding the mechanisms controlling intraplate seismicity and assessing the reactivation of inherited structure along the passive margins of the Eastern Seaboard and the Gulf of Mexico. For example, one of the key questions posed by the 2004 Earthscope Workshop: Research Frontiers in Appalachian Geology involved understanding the structures “associated with neotectonic activity in the Appalachians” ([http://www.earthscope.org/meetings/assets/ws\\_appalachian.php](http://www.earthscope.org/meetings/assets/ws_appalachian.php)). In addition to fault-related deformation, patterns of groundwater-related subsidence can also provide insight into fault geometries that may otherwise have very subtle surficial expression (i.e., beyond the detection of limits of satellite geodesy).

We suggest acquiring SAR imagery for the Central and Eastern United States that will focus on the seismicity in the New Madrid and Charleston regions, land subsidence mechanisms and fault mapping associated with differential motion across ground-water barriers in New York, Charleston, New Orleans, Galveston/Houston, and along the eastern coastal planes of the US. Advances in InSAR processing and analysis are now making it possible to image land surface deformation in the Central and Eastern US, where low deformation rates and temporal decorrelation have posed challenges in the past. To prove this concept, we have identified four primary targets (New Madrid, New Orleans, Galveston/Houston and Charleston) for routine imaging along with a broader swath encompassing several other major cities and scientific targets along the eastern seaboard.

#### New Madrid:

The New Madrid seismic zone in the central United States is the most seismically active intraplate region in North America with three widely felt magnitude 7-8 earthquakes ruptured along a 250 km long zone in the winter of 1811-1812 and an aftershock sequence that continues today. Recent analyses of continuous GPS stations around the New Madrid seismic zone seem to be resolving small deformations [e.g., *Smalley et al.*, 2005]. With the combination of almost a decade and a half of SAR imagery and new PSInSAR capabilities, it may be possible to utilize SAR imagery to measure the spatial and temporal variations in the strain field in the New Madrid Region as well as map possible structures associated with differential motion across ground-water barriers to better image the subsurface geology.

#### Rio Grande rift

The Rio Grande rift system in central New Mexico is one of the four large active continental rifts in the world, and the only major active rift in the continental US. The estimated extension rates range from sub-mm to 5 mm/yr, but uncertainties in measurements of total extension are

typically of the same order as the estimates themselves [Formento-Trigilio and Pazzaglia, 1998]. InSAR can provide critical constraints on strain rates within the rift zone, possible variations in extension rates along the rift zone, as well as shed light on proposed hypotheses of active versus passive rifting [e.g., Ruppel, 1995]. In the larger picture of understanding the dynamics of the plate boundary zone, resolving the kinematics across the Rio Grande rift zone is important on several accounts. Activity along the Rio Grande rift zone can influence the interpretation of all velocity vectors measured west of the rift zone (since many interpretations will hinge on estimates of motions in a North American reference frame). If the Rio Grande Rift is assumed to be inactive (equivalent to the assumption that the Colorado Plateau is not moving with respect to North America) then many of the inferred rates of deformation that lie west of the Colorado Plateau could be in error. In addition, the Rio Grande rift is associated with spectacular magmatic activity. The Socorro Magma Body, one of the largest active magma bodies ever documented in the continental crust is located within the rift proper at depth of about 20 km. Leveling data dating back to 1911 [Larsen *et al.*, 1998], and, more recently, InSAR observations [Fialko and Simons, 2001] revealed a broad uplift above the Socorro Magma Body at an average rate of 2-3 mm/yr. Frequent SAR acquisitions will allow us to establish whether the uplift continues, and indeed has a nearly constant rate. Immediately adjacent to the Rio Grande rift is the Valles caldera, a big neo-volcanic structure similar to Long Valley caldera in California and Yellowstone caldera in Wyoming, which was formed in the result of a catastrophic eruption about a million years ago. The data acquisition plan outlined in this report will help resolve key scientific questions related to interplay between mechanical extension and magmatism in a continental rift setting.

#### New Orleans:

In 2005 Hurricane Katrina underscored the vulnerability associated with land subsidence of coastal urban cities. The science rationale for New Orleans/Mississippi Delta is two fold: create a large archive of SAR imagery such that it is possible map the spatially and temporally varied subsidence patterns in an a region that has several large InSAR noise sources that make it difficult to image with differential InSAR, and understand and separate the deformation the mechanisms driving the motion. Locally, PSInSAR measurements in New Orleans reveal that some of the levee sections that failed during the hurricane had very high subsidence rates [Figure 7; Dixon *et al.*, 2006].

Regionally, subsidence has been associated with fluid pumping and sediment starvation from the Mississippi River. However, Dokka [2006] identified a tectonic source for costal subsidence in Louisiana with subsidence rates as high at 16.9 mm/yr. SAR imagery will provide the spatial density necessary to understand the complex deformation and separate various deformation mechanisms in the gulf coast region.

#### Galveston/Houston:

There is a long history of hydrocarbon and ground water pumping induced land subsidence in the Galveston/Houston region dating back to the early 1900s. InSAR has been used by multiple research groups to image subsidence throughout the region, with the conclusions that surface deformation can be measured with InSAR in humid environments and that the subsurface structures were complex [Stork and Sneed, 2002; Buckley *et al.*, 2003]. The InSAR imagery also identified active growth faults with vertical rates ranging between 0.5 to 4 cm/yr [Buckley *et al.*,

2003]. The science rationale is to further understand and model the mechanisms driving the large-scale regional subsidence and the development of growth faults. The high humidity, vegetation, and seasonal variability require frequent SAR acquisitions to minimize the noise.

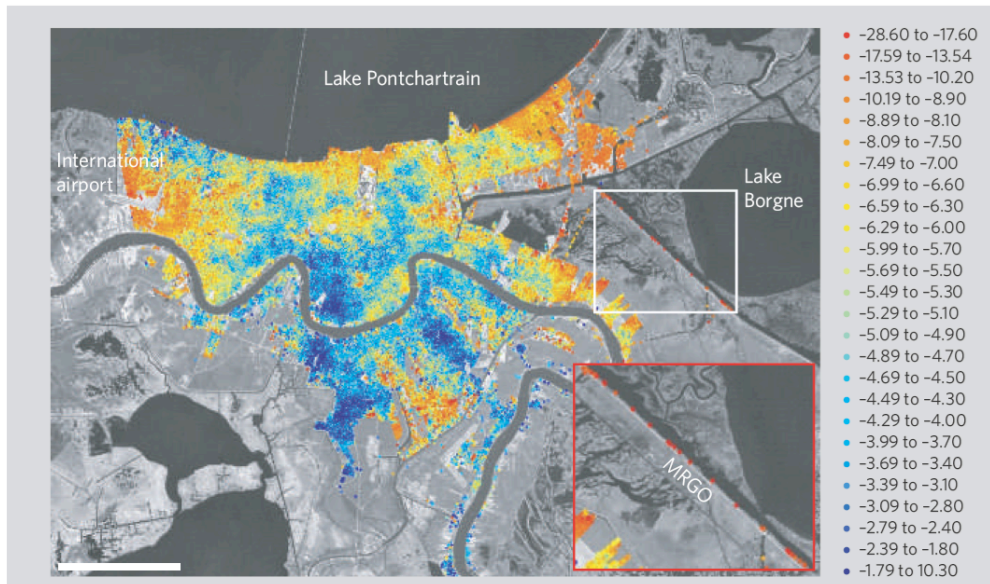


**Figure 7.** Map showing rate of subsidence for permanent scatterers in New Orleans and vicinity during 2002–05. Velocity values are given in millimeters per year as range change in the direction of radar illumination. Negative values indicate motion away from the satellite, consistent with subsidence. International airport, Louis Armstrong New Orleans International Airport; MRGO, Mississippi River–Gulf Outlet canal. Insets show location (white frame) and magnified view (red frame) of the region west of Lake Borgne, including eastern St Bernard Parish. Note the high rates of subsidence on the levee bounding the MRGO canal. Large sections of the MRGO levee were breached when Hurricane Katrina struck on 29 August 2005. Scale bar, 10 km. From *Dixon et al.*, [2006].

### Charleston:

The 1886 Charleston, South Carolina earthquake was one of the largest historic earthquakes in the eastern North America with an estimated magnitude between 6.6 and 7.3. While the damage was widespread, no surface faulting was reported for the earthquake. The subsurface faulting and subsurface structures are poorly known throughout the region. The science rationale is to develop a long-term SAR archive to image subsurface ground-water barriers that may be linked to the active regional tectonics and to characterize/model widespread ground water pumping induced subsidence in an eastern coastal aquifer. InSAR imagery has already been successfully applied to Charleston to map subsidence associated with aggressive ground water pumping [*Bawden et al.*, in preparation] and a comprehensive archive is needed to fully image both the subsidence and subsurface structures.

### Eastern coastal targets:

There are a number of science targets along the east coast of the US that could be routinely imaged with SAR satellite that would provide a wealth of information along a few descending swaths from Long Island, NY to Charleston, SC. Neotectonic studies have identified late Quaternary movements along key faults, such as the Norumbega fault in the northern

Appalachians, which may be related to present-day seismic activity. Additionally, InSAR imagery of subsurface ground-water barriers would help to resolve structures associated with the 1886 Charleston earthquake, the 1775 Cape Ann earthquake, Chesapeake Bay impact, and fault mapping in New York. Ground water induced subsidence has been observed in a number of coastal cities along the eastern US with preliminary InSAR analysis identifying subsidence in both Long Island/New York City and Charleston. Preliminary analysis shows InSAR-detectable deformation, but the number of scenes falls short of what is needed for a comprehensive analysis.

#### **4. Future Challenges and Scientific Justification for Continued Data Acquisitions**

The previous section highlighted the role of InSAR in revealing crustal deformation that simply could not be detected otherwise. In addition there have been numerous discoveries from a number of other areas and geological events. Example include small-scale yet pervasive displacements on faults adjacent to the main-shock rupture of the 1999, Izmit, Turkey, earthquake [Wright *et al.*, 2001], aseismic strain accumulation on active crustal faults [Burgmann *et al.*, 2000; Schmalzle *et al.*, 2006], and volcanic activity in remote or non-monitored areas [Amelung *et al.*, 2000; Pritchard and Simons, 2002, Wicks *et al.*, 2002]. The InSAR-derived displacement maps also allow detailed inferences about the amount and distribution of slip on earthquake faults [e.g., Jonsson *et al.*, 2002; Simons *et al.*, 2002; Fialko, 2004a], and the associated stress transfer within the seismically active crust [Masterlark and Wang, 2002; Pollitz *et al.*, 2001]. Knowledge of the co-seismic and post-seismic stress changes is also important for estimates of future seismic hazard.

Future challenges include (i) a routine retrieval of full 3-component vector displacement fields from InSAR observations from different vantage points, and (ii) a robust detection of subtle deformation, e.g., due to post-seismic relaxation transients or groundwater effects, as well as the interseismic strain accumulation leading up to earthquakes. The latter task will require processing of massively redundant InSAR acquisitions in order to suppress the observation noise (in particular, propagation effects), and push the accuracy of the InSAR technique to its theoretical limit of the order of millimeter-scale displacements over 10-km horizontal distances. Initial experiments with stacking of multiple interferograms [Peltzer *et al.*, 2001; Fialko and Simons, 2001; Lyons and Sandwell, 2003; Fialko, 2006] indicate that such accuracy is achievable with the existing data. Several groups are developing permanent scattering approaches to extract subtle crustal deformation in areas where decorrelation at C-band is severe. Other new technical developments can be expected as well. Recently, Bechor and Zebker [2006] presented a new method, Multiple Aperture InSAR, which can extract two components of deformation from a single pair of SAR images. It is difficult to predict what the future will bring in terms of techniques, but new technical developments always mean that additional value can be extracted from past data, and this emphasizes the need for the most complete possible data sets to be acquired, even when use of the data at present may appear to be difficult or limited.

Figure 8 shows the line-of-sight surface displacement field due to the postseismic relaxation following the 1992 magnitude 7.3 Landers earthquake in southern California, obtained from stacking of about 40 interferograms over a time period of 1992-1999. Future repeated SAR

acquisitions will be used in combination with continuous GPS measurements to address a number of outstanding problems including:

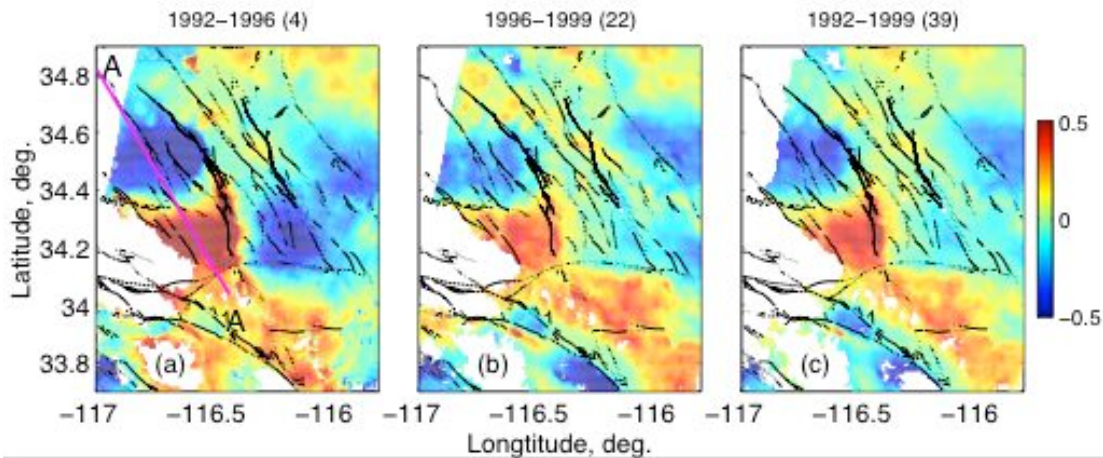


**Figure 8.** Stacked InSAR data from the *ERS* track127. Colors denote the average LOS velocities of the ground, in cm/yr, positive toward the satellite. Black wavy lines denote the Quaternary faults [Jennings, 1994]. Titles indicate the time period spanned by the interferometric stack, and numbers in the parentheses correspond to the number of interferograms in the stack. From Fialko [2004b].

*Postseismic deformation and stress transfer* – Frequent InSAR measurements may allow a robust determination of the mechanisms of post-seismic relaxation such as deep afterslip, poroelastic flow, or asthenospheric readjustment to the new stress field. Measuring and modeling this process will provide crucial insights into the overall rheological behavior of the Earth's crust and lithosphere, as well as into the suspected yet poorly understood relationships between the co- and post-seismic stress perturbations and triggered seismicity.

*Volcanic systems* - Similar approaches may be fruitful for studies of magma transport in the Earth's interiors and our understanding of the volcanic cycle [Wicks *et al.*, 1998; Dzurisin, 2003]. Little is known about deformation on many volcanoes in the Western US because only few of them are monitored. Because the magma-induced deformation might be in many ways simpler than that due to earthquakes, measurement of surface deformation in neovolcanic areas is an essential component of forecasting of potentially devastating eruptions. Numerous studies of particular volcanoes or eruptions show that it is possible to constrain the mechanisms driving the deformation and the geometry and location of magmatic sources at depth through a combination of highly accurate space geodetic observations and sophisticated numerical simulations [e.g., Lu *et al.*, 2000; Fialko *et al.*, 2001b; Wicks *et al.*, 2001; Mann and Freymueller, 2002; Lu *et al.*, 2005; Poland *et al.*, 2006]. An improved scientific understanding will also help in assessing the hazards posed by volcanic unrest. Ultimately, one might be able to discriminate a pre-eruptive activity from episodes of magmatic unrest that do not ultimately result in eruptions, which would mark both a great advance in our understanding of volcanic eruptions and a tremendous hazard mitigation tool. A continued acquisition of and access to the radar data is essential for monitoring the on-going deformation, testing and discriminating the existing models, and developing the new predictive capabilities. Specific data acquisition targets should include not only the volcanic systems instrumented by PBO, but all of the historically active volcanoes of the

Aleutian and Cascade arcs, as the utility of InSAR data is not dependent on the presence of equipment installed on the ground.

*Monitor crustal deformation on a continental scale* - One of the benefits of InSAR measurements is that wide-area coverage is available several times per year in almost any part of the Earth. The Plate Boundary Observatory will make continuous GPS measurements over the areas of highest tectonic strain but cannot provide an equally dense coverage over the broader areas of Western North America. Crustal deformation due to large earthquakes and volcanic activity can be monitored on a much wider scale if InSAR acquisitions are scheduled prior to an event.

### *Hydrology*

Natural and human-induced land-surface subsidence across the United States has affected more than 44,000 square kilometers in 45 states and is estimated to cost \$168 million annually from flooding and structural damage, with the actual cost significantly higher due to unquantifiable 'hidden costs' [*National\_Research\_Council*, 1991]. More than 80 percent of the identified subsidence in the United States is a consequence of the exploitation of underground water and the increasing development of land and water resources threatens to exacerbate existing land subsidence problems and initiate new ones [*Galloway et al.*, 1999]. Temporal and spatial changes in the surface elevation above aquifers provide important insights about the hydrodynamic properties of the underground reservoirs, the hydrologic structure of the aquifer, the potential infrastructure hazards associated with pumping, and effective ways to manage limited ground-water resources. InSAR as a technique has become a vital geodetic imaging tool for studying land-surface deformation associated with fluid pumping worldwide [*Alley et al.*, 2002; *Baer et al.*, 2001; *Bawden et al.*, 2001; *Galloway et al.*, 2002; *Sneed et al.*, 2003b; *Vasco et al.*, 2002; *Wicks et al.*, 1998]. Additionally, surface deformation associated with natural processes (e.g., sediment compaction, tectonic extension, sink hole collapse) and human activity (e.g., ground-water pumping, hydrocarbon extraction, geothermal production, mining) produce both vertical and horizontal motion that can readily be observed with InSAR imagery and with geodetic networks (Figure 9). By combining geodetic and hydrologic time-series data with the spatially dense InSAR imagery it is now possible to recognize and in some cases separate multiple sources of land-surface deformation at a given location.

Competing demands for water resources in the US have underscored the importance of ground-water supplies and the role of ground water in sustaining terrestrial ecosystems. More and more, ground-water systems are being used as a component of conjunctive-use strategies to optimize water availability by storing surplus water in subsurface reservoirs (aquifers) for use in peak-demand periods. These aquifer storage and recovery (ASR) practices create large changes in storage and in many places, concomitant deformation of the aquifer system. InSAR imagery is being used to provide valuable information about how aquifer systems respond to repeated stress conditions (seasonal pumping and recharge) thereby improving the scientific understanding of the mechanics of regional aquifer systems and improving the methods necessary to mitigate further loss in aquifer storage and permanent land-surface subsidence. Hydrocarbon and geothermal production also result in significant surface deformation that can be easily measured with InSAR, providing information on material that is difficult to obtain with other techniques. For example, *Fielding et al.* [1998] found that rapid and widespread subsidence in

the Los Hills and Beldridge oilfields in southern California impacted the flow gradient of the nearby California aqueduct in which the subsidence began reversing the water flow gradient.

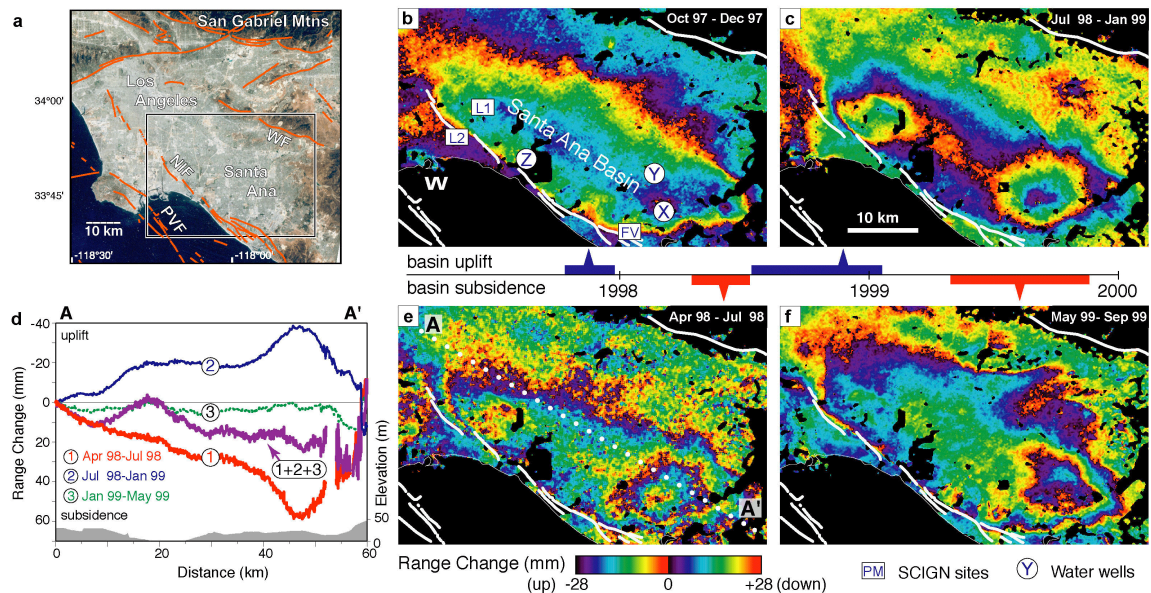


**Figure 9.** Seasonal deformation in the Santa Ana Basin. a, Location map for interferograms in Fig. 1 (black/white frame), and for Figs. 2 and 5 (full frame); Faults: PVF, Palos Verdes; NIF, Newport-Inglewood; and WF, Whittier. The time history bar in the center of the figure shows the period that each image spans, and summarizes the type of motion observed in the Santa Ana Basin. Blue bar denotes uplift (winter months) and red bar denotes subsidence (summer). b, October 1997 to December 1997. W, Wilmington oil field; L1, L2, and FV, are GPS sites; and X, Y, and Z locate water wells. c, July 1998 to January 1999 (175 days). f, May to October 1999 (105 days). e, April 1998 to July 1998 (105 days). d, Unwrapped range-change profiles along the Santa Ana Basin. Profile location a-a' is shown on e. The deformation is independent of topography, and is thus not an artifact of elevation-dependent atmospheric delays or an inaccurate digital elevation model. From *Bawden et al.*, [2001].

Similarly, InSAR has been used to image land subsidence associated with geothermal production worldwide. While the overall footprint of the subsidence associated with hydrocarbon and geothermal production is small, its impact can be significant. In the city of Long Beach, CA, extensive oil production has lowered the sections of this coastal city 8.8 meters since the pumping began in the 1920s, and has required extensive mitigation to prevent further damage from oceanic flooding. Oil production in Long Beach can still be seen today with about 3 cm of subsidence during a 70-day period in 1997 (see area W in Fig. 9b). InSAR provides scientists with new tools to understand the physical processes that result from the pumping and reinjection of fluids at depth in hydrocarbon and geothermal settings [e.g., *Fialko and Simons*, 2000].

### Landslides

Landslides are among the most widespread geologic hazards on Earth. Landslides cause billions of dollars in damages and thousands of deaths and injuries each year around the world. Landslides threaten lives and property in every State, resulting in an estimated 25 to 50 deaths and damage exceeding \$2 billion annually. Although most landslides in the United States occur as separate, widely distributed events, thousands of landslides can be triggered by a single severe storm or earthquake, causing spectacular damage in a short time over a wide area. The United States has experienced several catastrophic landslide disasters in recent years. In 1985, a massive

slide in southern Puerto Rico killed 129 people, the greatest loss of life from a single landslide in U.S. history. The 1982–83 and 1983–84 El Niño seasons triggered landslide events that affected the entire Western United States, including California, Washington, Utah, Nevada, and Idaho. The Thistle, Utah, landslide of 1983 caused \$400 million in losses, the most expensive single landslide in U.S. history, and the 1997–98 El Niño rainstorms in the San Francisco Bay area produced thousands of landslides, causing over \$150 million in direct public and private costs [Spiker and Gori, 2003].

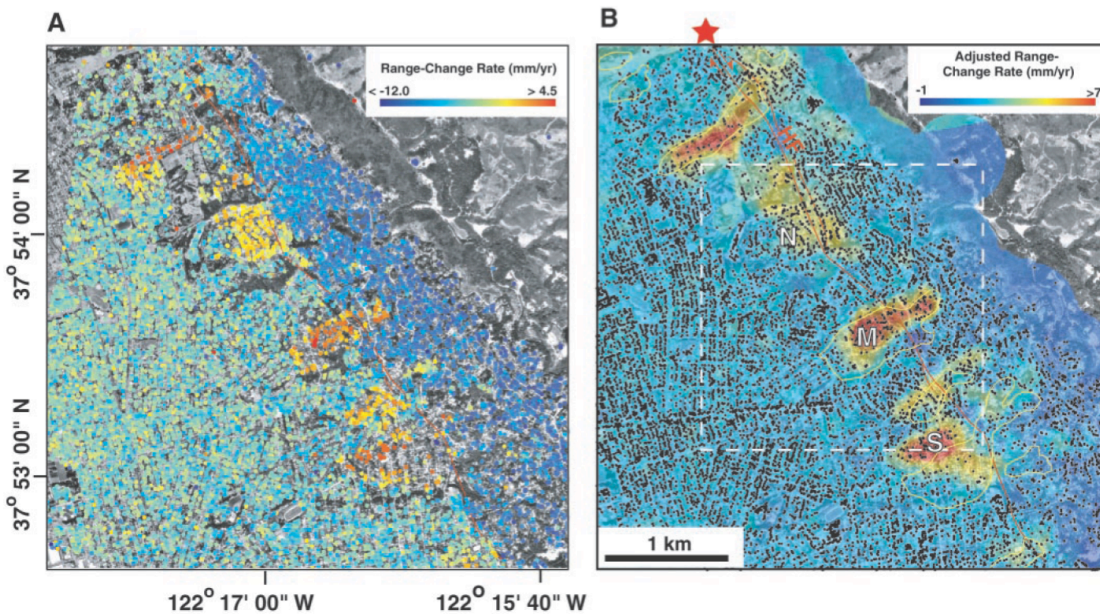


**Figure 10.** (A) Map view of PS-InSAR range-change rate measurements for the study area in the San Francisco Bay Area. Underlying image is an orthorectified air photo; Hayward Fault (HF) trace is indicated by a red line. (B) Map view of interpolated range-change rates (colors) adjusted for shallow creep (4 to 5 mm/year) along the HF. Yellow outlines show the location of mapped active landslides (14). Red star shows location of ML 4.1 earthquake on 4 December 1998 (8, 18). From Hilley *et al.*, [2004].

Recent advancements with InSAR process techniques, in particularly PSInSAR (Permanent Scatter InSAR), have now made it possible to track the movement of stable radar reflectors (rocks, buildings, etc.) in moderate to large-scale landslides. The PSInSAR technique provides a detailed time series for each of the stable reflectors such that differential motion across and along the landslide can be imaged and tracked through time. Hilley *et al.* [2004] used PSInSAR imagery to measure movements associated with slow-moving landslides. They found that PSInSAR was an effective tool at imaging temporally varied landslide slip rates associated with rainfall, shallow subsurface pore fluid pressure changes, and topography (Figure 10). Satellite SAR has become a valuable tool for tracking motion on major landslides and helping to understand the failure mechanisms.

#### *InSAR and PBO*

InSAR imagery has been an integral part of the Plate Boundary Observatory (PBO) GPS site selection process to ensure that the sites are located in areas with little known natural or human-induced surface motion associated with subsurface fluid flow and its management [Bawden *et al.*,

2005; Walls *et al.*, 2006]; continued satellite tasking and InSAR imagery analysis is needed to ensure that the full PBO network installation minimizes these effects. One of the objectives of the PBO is to measure very subtle transient and secular motion associated with tectonic and volcanic activity, however ground-water pumping has been shown to produce large horizontal and vertical motions in GPS time series that can be an order of magnitude or larger than the modeled surface motion from fault slip at depth [Bawden *et al.*, 2001; Watson *et al.*, 2002; Argus *et al.*, 1999]. Across the Los Angeles Basin, 29 of the 54 sites have either a ground water or hydrocarbon signature in their time-series that either mask or falsely accentuate the velocity field across this transpressional basin [Bawden *et al.*, 2001]. In many cases, simply relocating the site a few kilometers away from the pumping source significantly improves the quality of the GPS time series and helps to fulfill the science objectives.

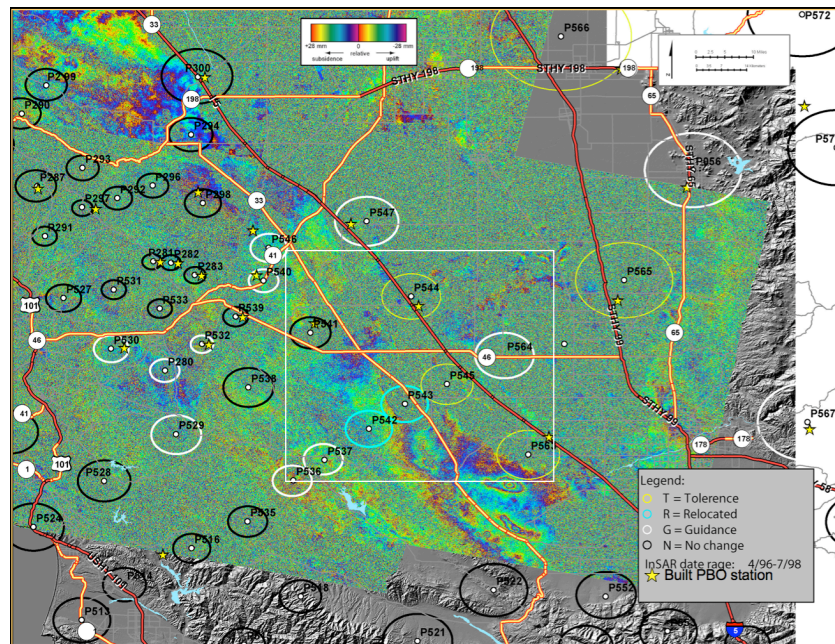


**Figure 11.** PBO site installations that were improved with InSAR imagery for one section of the California Central Valley.

Ground water pumping (both injection and extraction) and hydrocarbon production in the California Central Valley has made it difficult to locate potential PBO sites that are free of non-tectonic motion in their time-series and InSAR imagery has been used extensively to minimize these effects (Figure 11). InSAR has guided the installation of more than 100 PBO sites to date with more sites anticipated over the next two years.

Routine SAR satellite tasking of the PBO footprint is essential to fully understand and interpret the GPS time series. Once completed, PBO will be one of the densest geodetic networks in the world designed to image tectonic and volcanic deformation. However, natural and anthropogenic factors can produce inaccurate and often misleading trends in the time series for sites that are as close as a few kilometers apart. InSAR provides the spatially dense imagery needed to understand the full deformation process and source of non-tectonic deformation. For example, in December 2004 ten sites in the San Gabriel Valley California began moving radially outward with one site near the center moving upward a total of 4 cm. The initial interpretation

was a possible aseismic slip event in the vicinity of the Sierra Madre fault and was supported with a few small earthquakes near of the anomaly. However, a subsequent *Envisat* interferogram combined with ground-water well levels showed a broad region of uplift associated with the record rainfall (Figure 12). All of the horizontal and vertical motions could be explained as an elastic hydrologic response to a rapid influx of water into the local aquifer system [King *et al.*, 2005]. Additionally, the ever-increasing demand for ground-water resources has ushered in a new era of water mining throughout the west. The city of Las Vegas has purchased water rights for many of the basins in central Nevada and will begin pumping them soon.

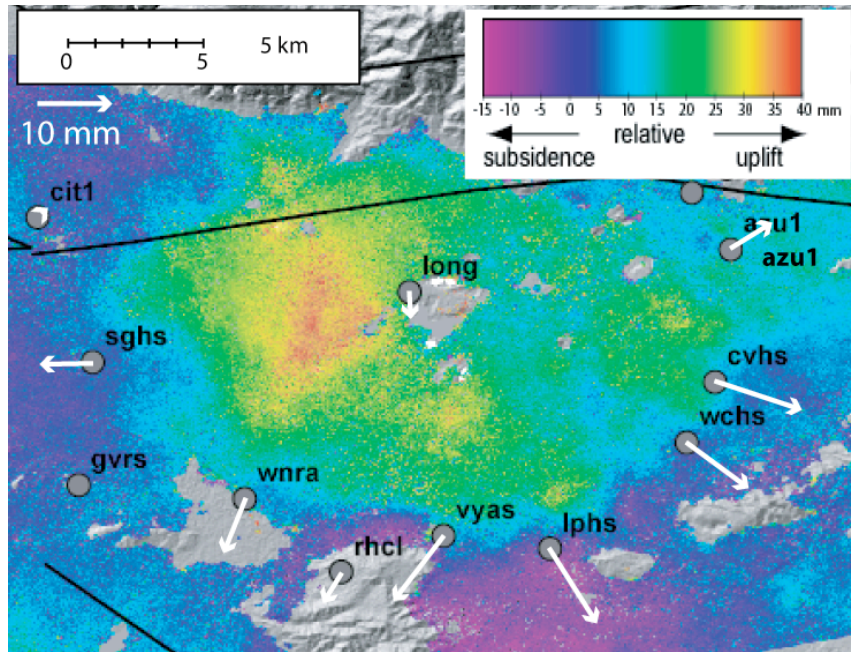


**Figure 12.** SCIGN GPS velocities on an Envisat interferogram for the winter/spring of 2005. Record rainfall during the winter/spring of 2005 uplifted the San Gabriel Valley by about 4 cm and moved the continuous GPS sites ringing the valley outward more than 1 cm (from King *et al.*, 2005).

Pumping in these basins will produce surface motion that will be difficult to recognize and correct in the low-strain-rate region with a sparse PBO footprint without the spatially dense InSAR imagery. Compounding the impact of water mining on PBO sites, concentrated pumping in central Nevada has been shown to produce bedrock subsidence that can be seen in a nearby GPS station velocity [Gourmelen and Amelung, 2005]. InSAR imagery provides the measurement density necessary to understand and account for spatially and temporally varying non-tectonic and non-volcanic deformation sources in the PBO time-series data. Continued SAR satellite tasking and archival analysis in the PBO footprint is necessary for the long-term success and interpretation of PBO data.

InSAR data also provide an excellent complement to PBO GPS time-series data at the volcanoes instrumented by PBO (Yellowstone, Long Valley, St. Helens, Augustine, Akutan, and Westdahl, Fisher and Shishaldin on Unimak Island). Volcanic deformation features have been observed at a wide variety of spatial scales, from long-wavelength signals caused by deep inflation or deflation [e.g., Wicks *et al.*, 2001; Lu *et al.*, 2002], to short-wavelength signals due to shallow inflation

magma sources and compaction of lava flows. For example, *Lu et al.* [2005] observed and modeled compaction of lava flows at Okmok volcano in the Aleutian arc due both to thermal compaction and to loading due to emplacement of lava from the more recent 1997 eruption. *Mann and Freymueller* [2003] identified a shallow contraction signal, inferred to be a contracting and degassing dike, at Fisher caldera on Unimak Island, Aleutian arc. The PBO GPS network cannot possibly be dense enough to guarantee detection and resolving power of deformation signals at all of these spatial scales, or to avoid aliasing of short-wavelength signals in a sparse network. Likewise, InSAR data cannot resolve change in deformation over days or hours, which can occur in the process of volcanic unrest or eruption [e.g., *Irwan et al.*, 2006].

## 5. Data requirements

The outlined plan will greatly facilitate and stimulate InSAR research within the EarthScope (and, more broadly, US) science community. The tasks are to acquire, archive, and distribute data as follows:

- Develop an ongoing acquisition plan for *Envisat*, *ALOS*, and *Radarsat-1* data over the regions of interest identified by the GeoEarthScope InSAR Working group (Figures 13 and 14);

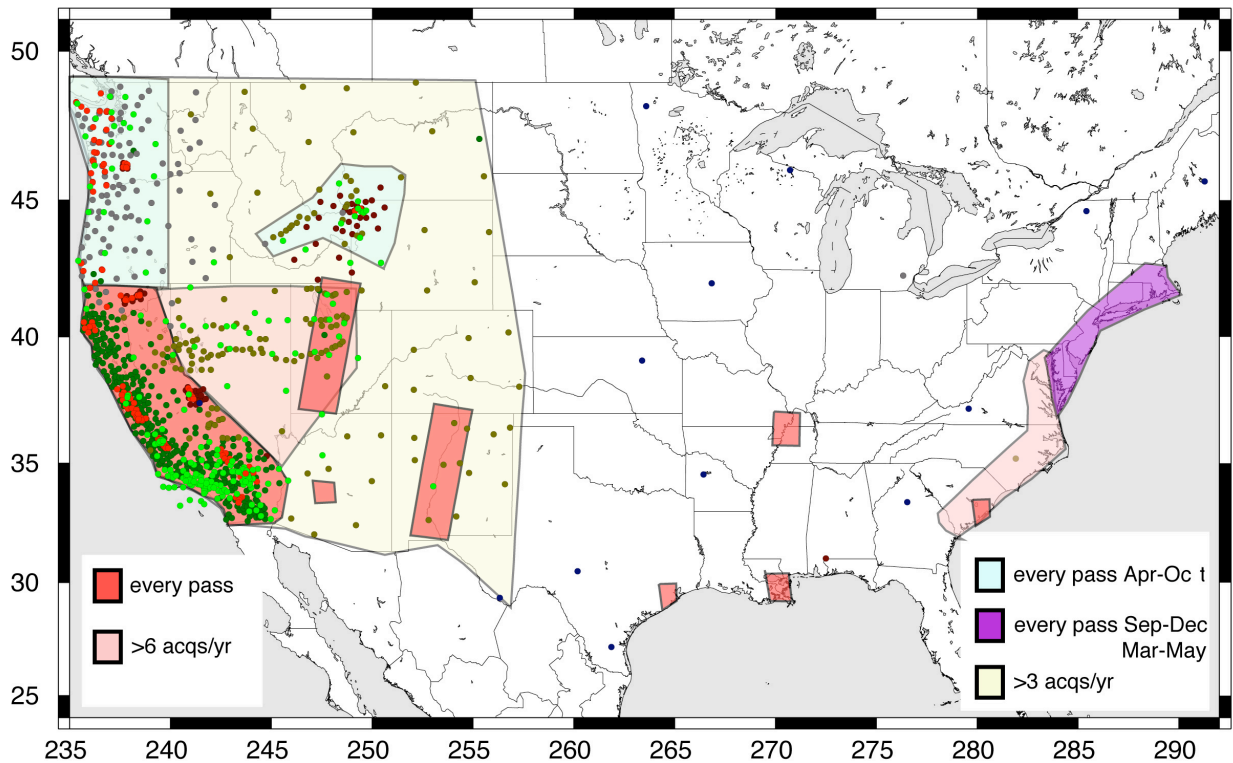


**Figure 13.** Geographic areas for acquisition of InSAR data from various available sensors. The hue of the area indicates the priority, frequency and timing of data acquisitions; red – highest priority, year-round acquisition; pink – high priority, acquire at least 7 scenes per year; blue - acquire data only during snow-free months; purple – acquire data during no snow/minimum vegetation season; yellow – acquire at least 4 scenes per year. Dots denote various ground-based instrumentation of PBO/EarthScope.

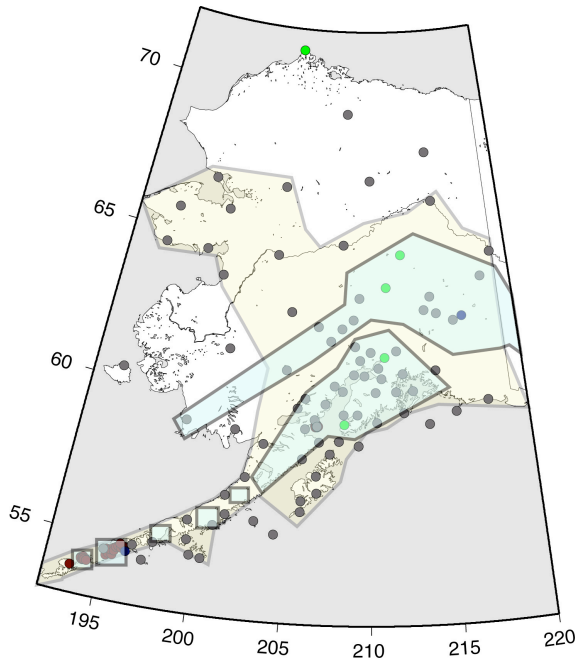


**Figure 14.** Same as in Figure 13, for the state of Alaska. Two other focus regions, the Fairweather fault in southeast Alaska and Okmok volcano in the Aleutian arc, are located outside the limits of this map.

- Acquire all available catalog data suitable for interferometry in the target areas to extend the temporal coverage (back to 1992 for the ERS data);
- Develop and implement a subsystem at UNAVCO for data delivery to GeoEarthScope, with a data search and order interface that includes selection by baselines values and an on-line L0 archive in a specified format;
- Develop a procedure for near real time (NRT) acquisition and processing for future *Envisat*, *ALOS*, *Radarsat-1* etc. data in the event of an earthquake. This includes re-programming of the satellite schedule (if necessary), negotiating foreign station NRT L0 delivery to the UNAVCO on-line archive, as well as utilizing existing ground stations in the US having the ability to downlink SAR data.

Most of the currently operational SAR platforms are capable of acquisitions in multiple modes (in particular, different look angles). For areas containing a significant historical archive, we recommend harmonizing future acquisitions with the dominant mode available in the archive. In addition to extending the time series of measurements, this will also minimize conflicts in future satellite tasking, as the historical data were requested by users interested in particular areas. In areas with a small or absent historical archive, we propose to acquire new data in standard swath 2 for *Envisat* (incidence angle of  $\sim 23^\circ$ ), and swath 6 for *Radarsat-1* (incidence angle of  $\sim 45^\circ$ ). We also emphasize the need for regular data takes from both the ascending and descending satellite passes. This will maximize the number of interferometric pairs for each instrument, reduce the effective repeat time (in case of a disaster event, the minimum revisit time), and provide four independent viewing geometry that will allow one to retrieve a full 3-component surface displacement field. The higher incidence angles provide a better sensitivity to the horizontal component of motion, and also increase the “critical baseline” with respect to a steeper-looking mode, thereby extending the number of potential interferometric matches.

Each data take is a swath of SAR data acquisition consisting of many 100km by 100km scenes. The total number of scenes acquired under the provisions of our plan will be of the order of  $10^5$ , which is approximately 50 times the size of the current WInSAR archive of *ERS-1/2* and *Envisat* data. This volume of data will require significant handling, from requests for acquisition to loading, ordering, and providing the user access to the Level 0 data.

The Level 0 data in the on-line archive will be in CEOS or Vexcel's Sky Telemetry Format. Some pre-processors will be used by the users of GeoEarthScope data to convert this format to the format needed for their respective Level 1 processing tools. A collection of relevant tools will be made available as open source code from the UNAVCO website.

### *Relationship to WInSAR*

The GeoEarthscope InSAR activities will be closely coordinated with the WInSAR consortium. All members of the InSAR working group are WInSAR members and the Chair is a member of WInSAR's executive committee. GeoEarthscope will enhance the WInSAR group with the professional support and operational framework. A synergy between WInSAR and GeoEarthScope will become especially productive now that both organizations are hosted by UNAVCO.

### *Priorities*

#### Infrastructure for the GeoEarthscope: Imagery portal/on-line data archive for all SAR platforms

An efficient use of massive SAR datasets that will be provided to the research community by UNAVCO requires a robust interface that would allow users to check the data availability for specific regions and radar platforms, interrogate metadata that are important for interferometric processing (in particular, the orbital baseline information), download the desired data, place new data requests, and check the existing ones. The InSAR Working Group considers the development and maintenance of such an interface one of the immediate and top priorities for UNAVCO.

#### Tasking & Acquisition of Future Data

Systematic acquisition of data is of paramount importance for InSAR studies of surface change. Frequent and consistent acquisitions of SAR imagery will enable studies of subtle yet important signals such as interseismic and postseismic deformation, slow inflation and deflation of magmatic bodies, migration of fluids at depth, etc. Also, such acquisitions will also greatly improve our ability to capture and characterize major disaster events such as large earthquakes, volcanic eruptions, and landslides. In addition, frequent data takes may enable studies of long-term surface deformation in more vegetated areas that have problems with maintaining correlation of radar images over time (for example, Northern California).

Below is a list of priorities and technical specifications for the GeoEarthScope acquisition plan. The order of items approximately reflects their priority within each category.

#### 1. New data:

1a. *Envisat* tasking for highest-priority Focus Areas (see Figure 13): data takes from every satellite pass, standard swath mode 2, VV polarization, from ascending and descending satellite orbits.

1b. *Envisat* Tasking for high-priority areas: same as 1a, with perhaps a lower acquisition rate; a minimum of 7 scenes should be acquired each year.

1c. *Envisat* tasking for high-priority areas with substantial winter snow cover; acquisitions are required on every pass during the snow-free season.

1d. Background tasking of *Envisat* over the rest of the PBO area (minimum of 3 data takes every year, same acquisition mode as in 1a-d).

1e. *ALOS* data acquisition and delivery (data acquisition modes defined by JAXA).

1f. *Radarsat-1* tasking and acquisition: same acquisition strategy as for 1a-1d, but in a different mode. We request standard swath 6, HH polarization, with acquisitions from both ascending and descending passes - unless significant amounts of data exist in a different mode for a given area (then continue acquisitions in that mode). This will be implemented through a collaboration between NASA, CSA, and ASF and incur no cost to GeoEarthScope. The InSAR Working Group expresses a strong interest in use of *Radarsat* data. The GeoEarthScope purchases of *Radarsat-1* data from the ASF should in general follow the policy and practice of WInSAR purchases from ESA.

1g. *ERS-2* tasking and acquisition – with somewhat improving Doppler control, some fraction of the new *ERS-2* may be suitable for interferometry. These data will be valuable in areas that maintain correlation over significant periods of time (>5 years, for example, in Southern California).

## 2. Catalog Acquisitions: High-priority areas

GeoEarthScope will acquire all historic data from the following sensors. This excludes data that are already present in the WInSAR archive.

2a. *Envisat* catalog

2b. *ERS* catalog

2c. *Radarsat* catalog

## 3. Catalog Acquisitions: Background (rest of Earthscope region; excluding data that are already present in the WInSAR archive).

3a. *Envisat* catalog

3b. *ERS* catalog

3c. *Radarsat* catalog

## **6. New and Emerging Technology**

Since the time that Earthscope was conceived and implementation began, the InSAR community has seen a rapid and exciting growth in new data processing and error mitigation techniques that have substantially expanded InSAR capability for monitoring time-dependent and spatially widespread geophysical signals. These techniques can be divided into three principal categories: 1) time series analysis using and ‘persistent scatterer’ approaches; 2) ScanSAR processing over swaths as wide as 400 km; and 3) atmospheric error mitigation using space-based sensors, numerical weather and digital elevation models, etc.

Because these new technologies offer the possibility of deepening the science contribution from InSAR in Earthscope, GeoEarthScope recommends that acquisition strategy takes into account these emerging technologies.

### PSInSAR & Time Series Analysis

The past several years have seen substantial development of InSAR time series techniques that enable the spatial resolving power of InSAR to be utilized over time-scales closer to continuous GPS [Berardino, et al., 2002; Lanari, et al., 2004] rather than yearly averages such as with previous ‘stacking’ techniques. Much of the technical advances have come from newly developed processing that utilizes the fact that for stable, point-like reflectors, minimal spatial decorrelation occurs and so interferometric phase may be interpreted even for data pairs with long perpendicular baselines that may exceed the critical baseline [Buckley, et al., 2004; Dixon, et al., 2006; Ferretti, et al., 2004; Ferretti, et al., 2001; Lyons and Sandwell, 2003; Hooper, et al., 2004; Werner, et al., 2003a,b]. Nomenclature for the new technique includes “permanent scatterers” [Ferretti, et al., 2001], “interferometric point target analysis (IPTA)” [Werner, et al., 2003a], and “persistent scatterers” [Hooper, et al., 2004], herein referred to as ‘PSInSAR’ techniques. For GeoEarthScope, one of the particularly attractive aspects of PSInSAR is that it enables much more thorough use of existing imagery catalogs.

### Atmospheric Mitigation

Despite these developments, little progress has been made in mitigating the impact of the atmosphere on SAR measurements and, for many times and locations the application of InSAR is limited by this noise source. Differential delays are primarily caused by changes in the distribution of water vapor in the atmosphere [Hanssen, 1998]. The radar signal is refracted by the atmosphere, and an increase in the amount of atmospheric water vapor between the acquisition times appears as an apparent increase in the distance to the ground surface, indistinguishable from real ground motion. Atmospheric effects can range over all wavelengths, with amplitudes up to several centimeters or even greater, leading to inevitable difficulties in identifying and interpreting deformation events captured with InSAR.

In fact, much of the interest in the PSInSAR techniques is due to their ability to provide details of the temporal evolution of deformation however both techniques achieve this through filtering procedures that assume statistical properties of the atmospheric component of the phase delays that are difficult to validate and may not be generally appropriate. Progress is just starting to be made at modeling the atmosphere in InSAR images based on concurrent observations [Webley, et al., 2002], weather models [Foster, et al., 2006] and space based instruments [Li, et al., 2005]. In order to further support the development of these mitigation techniques, which can eventually be used by the entire community, GeoEarthScope recommends the continual collection of images over areas (such as PBO high density areas) that have large amounts of CGPS sites where both deformation and atmospheric phases delays can be verified.

### ScanSAR

“ScanSAR”, or “wide swath” interferometry now makes it possible to form differential interferograms over areas much wider than the traditional ~100 x 100 km scene boundaries [e.g. Holzner and Bamler, 2002]. Currently it has been successfully undertaken in two modes: ScanSAR-ScanSAR and ScanSAR-StripMap. The former has been demonstrated with repeat passes for Radarsat-1 [Holzner and Bamler, 2002] and Envisat [Monti Guarnieri, 2004]. The Envisat example produced a deformation map of the Bam 2003 earthquake that had a width of ~400 km. In order to better take advantage of this new advance, ESA will attempt to provide better burst alignment information prior to the ordering of Envisat wide-swath data. Accordingly,

in order to investigate large spatial wavelength deformation signals in the PBO footprint, GeoEarthScope recommends the acquisition of wide-swath Envisat data on average once per year with the 50% overlap of the neighboring swaths.

### UAV SAR

Spaceborne SAR/InSAR can provide systematic coverage of the EarthScope region of interest with relatively wide swaths, but the repeat interval is fixed by orbital mechanics (i.e., 24-days for *Radarsat-1*, 35-days for *ERS-2* and *Envisat* ASAR, and 46-days for *ALOS PALSAR*) and subject to competing requirements that often mean that coverage of a given location cannot be obtained on every pass. These restrictions can limit the capacity of these systems to observe the dynamics of crustal deformation at shorter time scales before, during or after volcanic eruptions and earthquakes. Airborne SAR/InSAR can give us the experimental opportunity to monitor active seismic zones and volcanoes on a much more flexible basis and with greater spatial resolution. Such a capability would complement the data from the spaceborn SARs and thereby provide the opportunity to (1) respond to events, (2) monitor deformation hot spots on a more frequent basis and at higher spatial resolution, and (3) provide greater flexibility in viewing geometries thereby yielding more precise 3-D deformation.

NASA/JPL is currently developing a next-generation airborne L-band repeat-pass InSAR capability, known as UAVSAR, that is of great interest to GeoEarthScope. UAVSAR is being developed using a miniaturized and modular approach implemented with a pod design that is capable of being mounted on an unmanned aerial vehicle (UAV) suitable for long-duration flights in hazardous environments. The initial development, now underway, will mount UAVSAR on a NASA Gulfstream-3, which has greater access to airspace than UAVs at present. The UAVSAR incorporates modifications to the G-3 avionics allowing it to fly within a 10-meter tube (1-meter desired) under a variety of wind conditions and uses a phased array antenna that together will enable an unprecedented capability for repeat-pass InSAR. A second pod is being partially developed that could be used on the same (or another) aircraft to provide a highly flexible testbed for various cross-track, along-track, or bistatic imaging modes (or to provide even shorter revisit intervals than the 20-minutes required for a single aircraft to repeat a flight track). Flight tests of the UAVSAR will be conducted during FY07 and science demonstrations, including observations of deformation associated with volcanoes and seismic zones, will be conducted during much of FY08. Late in FY08 UAVSAR should become available for other experiments and operational use.

NASA views the UAVSAR as a testbed for a future US L-band InSAR mission and, as such, represents a NASA contribution to the EarthScope InSAR effort. NASA has expressed interest in making the UAVSAR available for use by EarthScope and is currently engaged in developing potential scenarios for such use as part of its advance planning process.

GeoEarthScope recommends that NSF engage NASA in discussions on potential use of UAVSAR for EarthScope to include monitoring of selected volcanic and seismic zones and event-driven response to hot spots. The GeoEarthScope InSAR working group will support this effort by developing a set of optional scenarios for experimental/operational use of UAVSAR. These options can then be used by NSF and NASA to assess the potential benefits, costs and associated schedule impacts.

## 7. Budget Justification

Our data acquisition plan includes essentially all available SAR imagery that is suitable for interferometry in the primary target areas of PBO and EarthScope. The highest priority is tasking of the currently operational SAR satellites. For Envisat, the estimated cost of tasking is \$160k/year in high priority areas (every possible data take, see Figure 13), and \$60k/year in the rest of the PBO/EarthScope area (“background” acquisition mode). This amounts to a total of \$660k over three years of the GeoEarthScope funding period. This estimate is based on the acquisition strategy outlined in Section “Priorities” and in Figure 13, assuming the average cost of \$125 per strip of 4 standard frames (400 km x 100 km); these costs include data delivery. The *Radarsat-1* tasking will be implemented through a collaboration between NASA, ASF, and CSA, and incur no cost to GeoEarthScope. The Working Group recommends that a sub-committee formed from the Group members takes part in communications with the scheduling segment of the *Radarsat* mission, and oversees the delivery of new *Radarsat* data to UNAVCO. The next highest priority is an acquisition of the historical catalog data from the existing missions. The largest item is the ESA catalog (including both *ERS-1,2* and *Envisat* catalogs, excluding data that have been already acquired through WInSAR). The estimated cost is \$608k, based on the total area of interest, and the assumed average of 4 data takes per year. The delivery of new *ALOS*, and catalog *Radarsat-1* data is currently proposed via a collaboration with the Alaska SAR Facility (ASF). The costs (\$150k/yr for the upcoming *ALOS* data, and \$162k for the *Radarsat* catalog) are a fraction of total costs involved in the data delivery from ASF. The remaining costs will be covered by NASA. The Working Group recommends that the GeoEarthScope purchases of *ALOS* and *Radarsat-1* data from the ASF follow the policy and practice of data acquisitions from ESA. Also, a survey of available commercial vendors shall be undertaken to establish the most efficient way of acquiring the new *ALOS* data; GeoEarthScope may solicit proposals from potential data suppliers to select an optimal route for the efficient data delivery. The main expense items are summarized in the following table.

Area/Item	per year	over 3 years	total (\$M)
<b>Western US</b>			
Background Tasking Envisat	60000	180000	<b>1.88</b>
ESA Catalog (1992-2006)	608000	608000	
ALOS	150000	450000	
RADARSAT Catalog	162000	162000	
<b>Focus areas</b>			
(high-priority Envisat tasking)	160000	480000	
San Andreas System			
ECSZ			
Garlock			
Walker Lane			
Mendocino Triple Junction			
Long Valley			
Yellowstone			
Cascadia Volcanoes			
Cascadia Subduction Zone			
Cascadia Forearc			

Denali Fault  
Alaska Volcanoes  
Southern Alaska Subduction  
Zone  
Rio Grande Rift  
Wasatch  
Las Vegas  
Houston  
New Orleans  
Central Valley

## 8. References

- Alley, W. M., R. W. Healy, J. W. LaBaugh, and T. E. Reilly, Flow and Storage in Groundwater Systems, *Science*, 296, 1985 – 1990, doi: 10.1126/science.1067123, 2002.
- Amelung, F., S. Jonsson, H. Zebker and P. Segall, Widespread uplift and trap door faulting on Galápagos volcanoes observed with radar interferometry. *Nature*, Volume 407 No. 6807, p. 993-996, 2000.
- Argus, D. F., M. B. Heflin, and J. F. Zumberge, Shortening and thickening of metropolitan Los Angeles measured and inferred by using geodesy, *Geology*, 27, 703, 1999.
- Atwater, B. F., and E. Hemphill-Haley, Recurrence intervals for great earthquakes of the past 3,500 years at northeastern Willapa Bay, Washington, *USGS Professional Paper 1576*, 1997.
- Baer, G., U. Schattner, D. Wachs, D. Sandwell, S. Wdowinski and S. Frydman, The lowest place on Earth is subsiding—An InSAR (interferometric synthetic aperture radar) perspective, *GSA Bulletin*, 114, 12-23, 2002.
- Bawden, G. W., W. Thatcher, R. S. Stein, K. W. Hudnut and G. Peltzer, Tectonic contraction across Los Angeles after removal of groundwater pumping effects, *Nature*, 412, pp. 812-815, 2001.
- Bechor, N. B. D., and H. A. Zebker, Measuring two-dimensional movements using a single InSAR pair, *Geophys. Res. Lett.*, 33, L16311, doi:10.1029/2006GL026883, 2006.
- Berardino, P., et al. (2002), A new algorithm for surface deformation monitoring based on small baseline differential SAR interferograms, *IEEE Trans. Geosci. Remote Sens.*, 40, 2375– 2383.
- Buckley, S. M., P. A. Rosen, S. Hensley, and B. D. Tapley, Land subsidence in Houston, Texas, measured by radar interferometry and constrained by extensometers, *J. Geophys. Res.*, 108, 2542, doi:10.1029/2002JB001848, 2003.
- Buckley, S. M., et al. (2004), Next-Generation InSAR Ground-Truth Data and Techniques: Initial Results, paper presented at 26th Seismic Research Review - Trends in Nuclear Explosion Monitoring, Orlando, Florida.
- Dixon, T. H., et al., Subsidence and flooding in New Orleans, *Nature*, 441, 587-588, 2006.
- Dokka, R. K., Modern-day tectonic subsidence in coastal Louisiana, *Geology*, 34, 281-284, doi:10.1130/G22264.1, 2006.
- Dragert, H., R.D. Hyndman, G.C. Rogers, and K. Wang, Current deformation and the width of the seismogenic zone of the northern Cascadia subduction thrust, *J. Geophys Res*, 99, 653-668, 1994.
- Dzurisin, D., A comprehensive approach to monitoring volcano deformation as a window on the eruption cycle, *Rev. Geophys.*, 41(1), 1001, doi:10.1029/2001RG000107, 2003.
- Ferretti, A., et al. (2004), InSAR permanent scatter analysis reveals ups and downs in San Francisco Bay area, *EOS*, 85.

- Ferretti, A., et al. (2001), Permanent Scatterers in SAR Interferometry, *IEEE Trans. Geosci. Remote Sensing*, 39, 8-20.
- Fialko, Y., and M. Simons, Deformation and seismicity in the Coso geothermal area, Inyo County, California: Observations and modeling using satellite radar interferometry, *J. Geophys. Res.*, 105, 21,781-21,794, 2000.
- Fialko, Y., and M. Simons, Evidence for on-going inflation of the Socorro magma body, New Mexico, from Interferometric Synthetic Aperture Radar imaging, *Geophys. Res. Lett.*, 28, 3549-3552, 2001.
- Fialko, Y., M. Simons, and D. Agnew, The complete (3-D) surface displacement field in the epicentral area of the 1999 Mw7.1 Hector Mine earthquake, California, from space geodetic observations, *Geophys. Res. Lett.*, 28, 3063-3066, 2001a.
- Fialko, Y., M. Simons, and Y. Khazan, Finite source modeling of magmatic unrest in Socorro, New Mexico, and Long Valley, California, *Geophys. J. Int.*, 146, 191-200, 2001b.
- Fialko, Y., D. Sandwell, D. Agnew, M. Simons, P. Shearer, and B. Minster, Deformation on nearby faults induced by the 1999 Hector Mine earthquake, *Science*, 297, 1858-1862, 2002.
- Fialko, Y., Probing the mechanical properties of seismically active crust with space geodesy: Study of the co-seismic deformation due to the 1992 Mw7.3 Landers (southern California) earthquake, *J. Geophys Res.*, 109, B03307, doi:10.1029/2003JB002756, 2004a.
- Fialko, Y., Evidence of fluid-filled upper crust from observations of post-seismic deformation due to the 1992 Mw7.3 Landers earthquake, *J. Geophys Res.*, 109, B08401, doi:10.1029/2003JB002985, 2004b.
- Fialko, Y., D. Sandwell, M. Simons, and P. Rosen, Three-dimensional deformation caused by the Bam, Iran, earthquake and the origin of shallow slip deficit, *Nature*, 435, doi:10.1038/nature03425, 295-299, 2005.
- Fialko, Y., Interseismic strain accumulation and the earthquake potential on the southern San Andreas fault system, *Nature*, 441, doi:10.1038/nature04797, 968-971, 2006.
- Fielding, E. J., Blom, R. G. , and Goldstein, R. M., Rapid subsidence over oil fields measured by SAR interferometry, *Geophys. Res. Lett.* Vol. 25, 3215 (98GL52260), 1998.
- Formento-Trigilio, M.L., Pazzaglia, F.J., Tectonic geomorphology of the Sierra Nacimimiento: Traditional and new techniques in assessing long-term landscape evolution in the southern Rocky Mountains, *Journal of Geology*, 106, 433-453, 1998.
- Foster, J., et al. (2006), Mitigating atmospheric noise for InSAR with a high resolution weather model, *Geophys. Res. Lett.*, accepted.
- Freed, A. M., R. Bürgmann, E. Calais, J. Freymueller, and S. Hreinsdóttir (2006), Implications of Deformation Following the 2002 Denali, Alaska Earthquake for Postseismic Relaxation Processes and Lithospheric Rheology, *J. Geophys. Res.*, doi:10.1029/2005JB003894.
- Goldfinger, C., Nelson, C.H., and Johnson, J.E., Holocene earthquake records from the Cascadia subduction zone and northern San Andreas fault based on precise dating of offshore turbidites, *Annual Review of Earth and Planetary Sciences*, 31, 555-577, 2003.
- Gourmelen, N. and F. Amelung, Post-seismic mantle relaxation in the Central Nevada Seismic Belt, *Science* 310: 1473-1476 [DOI: 10.1126/science.1119798], 2005.
- Hanssen, R. (1998), Atmospheric heterogeneities in ERS tandem SAR interferometry, 136 pp, Delft University Press, Delft.
- Hilley, et al., Dynamics of slow-moving landslides from permanent scatterer analysis, *Science*, 304, 1952-1955, 2004.
- Holzner, J., and R. Bamler, Burst-mode and ScanSAR interferometry, *Geoscience and Remote Sensing, IEEE Trans.*, 40, 1917-1934, 2002.

Hooper, A., et al. (2004), A new method for measuring deformation on volcanoes and other natural terrains using InSAR persistent scatterers, *Geophys. Res. Lett.*, *31*, doi:10.1029/2004GL021737.

Irwan, M., Kimata, F., Fujii, N., Time-dependent modeling of magma intrusion during the early stage of the 2000 Miyakejima activity. *Journal of Volcanology and Geothermal Research* *150*, 202– 212, doi:10.1016/j.jvolgeores.2005.07.014, 2006.

Jacobs, A., D. Sandwell, Y. Fialko, and L. Sichoix, The 1999 (M<sub>w</sub>7.1) Hector Mine, California, earthquake: Near-field postseismic deformation from ERS interferometry, *Bull. Seis. Soc. Am.*, *92*, 1433-1442, 2002.

Jennings, C., *Fault activity map of California and adjacent areas, with locations and ages of recent volcanic eruptions*, California Division of Mines and Geology, Geologic Data Map No. 6, map scale 1:750,000, 1994.

Jonsson, S., H. Zebker, P. Segall, and F. Amelung, Fault Slip Distribution of the 1999 Mw 7.1 Hector Mine, California, Earthquake, Estimated from Satellite Radar and GPS Measurements, *Bull. Seis. Soc. Am.*, *92*, 1377 - 1389, 2002.

Khazaradze, G., A. Qamar, and H. Dragert, Tectonic deformation in western Washington from continuous GPS measurements, *Geophys. Res. Lett.*, *26*, 3153-3156, 1999.

King et al., A GPS Anomaly in the San Gabriel Valley, California, *Proc. Annual SCEC meeting*, Palm Springs, CA, 2005.

Lanari, R., et al., Satellite radar interferometry time series analysis of surface deformation for Los Angeles, California, *Geophys. Res. Lett.*, *31*, L23613, 2004.

Larsen, S., R. Reilinger, and L. Brown, Evidence of ongoing crustal deformation related to magmatic activity near Socorro, New Mexico, *J. Geophys. Res.*, *91*, 6283-6293, 1986.

Li, Z., et al. (2005), Interferometric synthetic aperture radar (InSAR) atmospheric correction: GPS, Moderate Resolution Imaging Spectroradiometer (MODIS), and InSAR integration, *Journal of Geophysical Research*, *110*.

Lorenzetti, E. and T. E. Tullis, Geodetic predictions of a strike-slip fault model: Implications for intermediate- and short-term earthquake prediction, *J. Geophys. Res.*, *94*, 12343-12361, 1989.

Lu, Z., C. Wicks Jr., J. A. Power, and D. Dzurisin (2000), Ground deformation associated with the March 1996 earthquake swarm at Akutan volcano, Alaska, revealed by satellite radar interferometry, *J. Geophys. Res.*, *105*, 21,483–21,496.

Lu, Z., C. Wicks Jr., D. Dzurisin, J. A. Power, S. C. Moran, and W. Thatcher (2002), Magmatic inflation at a dormant stratovolcano: 1996–1998 activity at Mount Peulik volcano, Alaska, revealed by satellite radar interferometry, *J. Geophys. Res.*, *107*, 2134, doi:10.1029/2001JB000471.

Lu, Z., T. Masterlark, and D. Dzurisin (2005), Interferometric synthetic aperture radar study of Okmok volcano, Alaska, 1992–2003: Magma supply dynamics and postemplacement lava flow deformation, *J. Geophys. Res.*, *110*, B02403, doi:10.1029/2004JB003148.

Lyons S., and D. Sandwell, Fault creep along the southern San Andreas from interferometric synthetic aperture radar, permanent scatterers, and stacking, *J. Geophys. Res.*, *108*, B2047, doi:10.1029/2002JB001831, 2003.

Mann, D., J. T. Freymueller, and Z. Lu, Deformation associated with the 1997 eruption of Okmok volcano, Alaska, *J. Geophys. Res.*, 2001JB000163, 2002.

Mann, D., and J. Freymueller, Volcanic and tectonic deformation on Unimak Island in the Aleutian Arc, Alaska, *J. Geophys. Res.*, *108*(B2), 2108, doi:10.1029/2002JB001925, 2003.

Massonnet, D., W. Thatcher, and H. Vadon, Detection of postseismic fault-zone collapse

following the Landers earthquake, *Nature*, 382, 612–616, 1996.

Masterlark, T., and H. Wang, Transient stress-coupling between the 1992 Landers and 1999 Hector Mine, California, earthquakes, *Bull. Seism. Soc. Am.*, 92, 1470–1486, 2002.

McCaffrey, R., M. D. Long, C. Goldfinger, P. Zwick, J. Nabelek, and C. Smith, Rotation and plate locking at the southern Cascadia subduction zone, *Geophysical Research Letters*, 27, 3117–3120, 2000.

McCaffrey, R., Crustal block rotations and plate coupling, in *Plate Boundary Zones*, S. Stein and J. Freymueller, editors, AGU Geodynamics Series 30, 101–122, 2002.

Meilano I., F. Kimata and N. Fujii, Time dependent modeling of magma intrusion during the early stage of the 2000 Miyakejima activity, *Journal of Volcanology and Geothermal Research*, 150, Issues 1-3, The Changing Shapes of Active Volcanoes - Recent Results and Advances in Volcano Geodesy, 202–212. 2006.

Mitchell, C.E., P. Vincent, R.J. Weldon, and M.A. Richards, Present day vertical deformation of the Cascadia margin, Pacific Northwest, United States, *J. Geophys. Res.*, 99, 12257–12277, 1994.

Nelson, A.R., Jennings, A.E., and Kashima, K., An earthquake history derived from stratigraphic and microfossil evidence of relative sea level change at Coos Bay, southern coastal Oregon, *Geological Society of America Bulletin*, 108, 141–154, 1996.

Peltzer, G., F. Crampe, S. Hensley, and P. Rosen, Transient strain accumulation and fault interaction in the Eastern California shear zone, *Geology*, 29, 975–978, 2001.

Poland, M., Burgmann, R., Dzurisin, D., Lisowski, M., Masterlark, T., Owen, S., and Fink, J., *Journal of Volcanology and Geothermal Research*, 150, 55, 2006.

Pollitz, F. F., C. Wicks, W. Thatcher, Mantle Flow Beneath a Continental Strike-Slip Fault: Postseismic Deformation After the 1999 Hector Mine Earthquake, *Science*, 293, 1814–1818, 2001.

Pollitz, F. F., Transient rheology of the uppermost mantle beneath the Mojave Desert, California, *Earth Planet. Sci. Lett.*, 215, 89–104, 2003.

Pritchard, M. E. and M. Simons, A satellite geodetic survey of large-scale deformation of volcanic centres in the central Andes. *Nature*, 418, 167–171, 2002.

Rundle, J. B. and D. D. Jackson, Numerical simulation of earthquake sequences, *Bull. Seis. Soc. Am.*, 67, 1363–1377, 1977.

Ruppel, C., Extensional processes in continental lithosphere, *J. Geophys. Res.*, 100, 24,187–24,215, 1995.

Rymer, M. J., V. E. Langenheim, and E. Hauksson, The Hector Mine, California, Earthquake of 16 October 1999: Introduction to the Special Issue, *Bull. Seis. Soc. Am.*, 92, 1147 - 1153, 2002.

Satake, K., Shimazaki, K., Tsuji, Y., and Ueda, K., Time and size of a giant earthquake in Cascadia inferred from Japanese tsunami records of January 1700, *Nature*, 379, 246–249, 1996.

Savage, J. C., Equivalent strike-slip earthquake cycles in half-space and lithosphere-asthenosphere earth models, *J. Geophys. Res.*, 95, 4873–4879, 1990.

Savage, J.C., M. Lisowski, and W.H. Prescott, Strain accumulation in western Washington, *J. Geophys. Res.*, 96, 14,493–14,507, 1991.

Shen, Z., D. Jackson, Y. Feng, M. Cline, M. Kim, P. Fang, and Y. Bock, Postseismic deformation following the Landers earthquake, California, 28 June 1992, *Bull. Seism. Soc. Am.*, 84, 780–791, 1994.

Simons, M., Y. Fialko, and L. Rivera, Co-seismic static deformation from the 1999 M<sub>w</sub>7.1 Hector Mine, California, earthquake, as inferred from InSAR and GPS observations, *Bull. Seis. Soc. Am.*, 92, 1390–1402, 2002.

Smalley, R., M. A. Ellis, J. Paul, and R. B. Van Arsdale, Space geodetic evidence for rapid strain rates in the New Madrid seismic zone of central USA, *Nature*, 435, 1088-1090, 2005.

Spiker, E. C. and Gori, P. L., National landslide hazards mitigation strategy—a framework for loss reduction., *U.S. Geological Survey Circular 1244*, 4-13, 2003.

Stork, S.V., and Sneed, M., Houston-Galveston Bay area, Texas, from space—A new tool for mapping land subsidence, *U.S. Geological Survey Fact Sheet 110–02*, 6 p., 2002.

Thatcher, W., Nonlinear strain buildup and the earthquake cycle on the San Andreas fault: *J. Geophys. Res.*, 88, 5893-5902, 1983.

Tse, S. T. and J. R. Rice, Crustal earthquake instability in relation to the depth variation of frictional slip properties, *J. Geophys. Res.*, 91, 9452-9472, 1986.

Turcotte, D. L. and G. Schubert, *Geodynamics*, 2nd edn, Cambridge Univ. Press, New York, 2002.

Vasco, D. W., C. Wicks, K. Karasaki, and O. Marques, Geodetic imaging: reservoir monitoring using satellite interferometry. *Geophysical Journal International*, 149, 555-571, doi: 10.1046/j.1365-246X.2002.01569.x. 2002.

Watson, K. M., Y. Bock, and D. T. Sandwell, Satellite interferometric observations of displacements associated with seasonal groundwater in the Los Angeles Basin, *J. Geophys. Res.*, 107, doi: 10.1029/2001JB000470, 2002.

Webley, P. W., et al. (2002), Atmospheric water vapour correction to InSAR surface motion measurements on mountains: results from a dense GPS network on Mount Etna, *Physics and Chemistry of the Earth, Parts A/B/C*, 27, 363-370.

Werner, C., et al. (2003a), Interferometric Point Target Analysis for Deformation Mapping, paper presented at IGARSS'03, Toulouse, France.

Werner, C., et al. (2003b), Interferometric Point Target Analysis with JERS-1 L-band SAR Data, paper presented at IGARSS'03, Toulouse, France.

Wicks, C. Jr., W. Thatcher and D. Dzurisin, Migration of fluids beneath Yellowstone Caldera inferred from satellite radar interferometry, *Science*, 282, 458-462, 1998.

Wicks, C. W., Jr., D. Dzurisin, S. Ingebritsen, W. Thatcher, Z. Lu, and J. Iverson, Magmatic activity beneath the quiescent Three Sisters volcanic center, central Oregon Cascade Range, USA, *Geophys. Res. Lett.*, 29, 1122, doi:10.1029/2001GL014205, 2002.